Environmental Nanotechnology, Monitoring & Management 18 (2022) 100673

Contents lists available at ScienceDirect

Environmental Nanotechnology, Monitoring & Management

journal homepage: www.elsevier.com/locate/enmm

A critical review on graphene oxide nanostructured material: Properties, Synthesis, characterization and application in water and wastewater treatment

O.J. Ajala [a,c,*], J.O. Tijani [a,c], M.T. Bankole [a,c], A.S. Abdulkareem [b,c]

[a] Department of Chemistry, Federal University of Technology, P. M. B. 65, Bosso Campus, Minna, Niger state, Nigeria
[b] Department of Chemical Engineering, Federal University of Technology, P. M. B. 65, Gidan Kwano Campus, Minna, Niger State, Nigeria
[c] Nanotechnology Research group, Africa Center of Excellence for Mycotoxin and Food Safety, Federal University of Technology, Minna, P. M. B. 65, Niger State, Nigeria

ARTICLE INFO

Keywords:
Graphene
Graphene oxide
Advanced oxidation process
Hybrid advanced oxidation process

ABSTRACT

Graphene oxide is an emerging nanomaterial with diverse applications for energy storage, conversation (electrodes) and industrial wastewater treatment (adsorbent and photocatalysts) because of their outstanding electrical, thermal and chemical properties. In view of this background, this review paper examines the properties, preparation methods and characterization techniques for graphene oxide (GO) nanostructured materials. A brief strategy for improving GO efficiency such as doping/co-doping GO with selected heterogeneous semiconductor metal oxides was provided. The immobilisation of GO with a high bandgap material resulting to the shifting of absorption threshold to the visible region and enhancement of photoactivity performance were also discussed. The application of GO based nanomaterial in Fenton like reaction, ozonation, photocatalysis, photo-Fenton, photoelectrocatalysis and combination of photocatalysis and photon-Fenton for water treatment applications were provided. The presence of graphene oxide nanostructured materials in composite material enhanced the overall performance in their respective applications. Finally, the review provides insight into future perspectives and improvements especially the scaling up of graphene oxide based nanocomposites based technology for industrial wastewater treatment.

1. Introduction

Graphene is a two dimensional (2D) hexagonal structure material covalently bonded to a single sheet of atomic thickness similar to chain of polycyclic aromatic hydrocarbon in a honey comb crystal lattice with a unit cell of two carbon atoms (Lingamdinne et al., 2019). Since 2004, graphene material has been utilized for lithium-ion batteries (LIBs) by researchers due to its unique electrochemical and physical properties. Additionally, Graphene possesses excellent thermal conductivity, surface to volume ratio, mechanical strength, transparency and quantum electro-dynamic among others, thus makes it one of the most studied and exciting nanomaterials to emerge in 21st century (Gupta, 2018). Graphene has found application in different fields of science and engineering such as; fuel cells, energy storage devices, sound transducers, electromagnetic shielding (Lingamdinne et al., 2019), Other application of graphene include; biosensors, aerospace, photonic, organic light emitting diodes, integrated circuits, protective coatings, biomedical decontamination devices (Ray, 2015). The relative electron in graphene can travel close to light speed and it is termed Dirac fermions (Li, 2018). According to Vidhya *et al.,* (Vidhya, 2020) graphene is a pseudocapacitive materials and a building block of the other graphitic allotropes owing to its excellent large surface area, high conductivity and good mechanical property. Thus, Graphene can be used to enhance the properties of the composite material.

Various methods have been used to synthesis graphene, graphite, non-graphitic carbon and carbon-containing materials. These methods are classified into top-down and bottom-up approaches (Kumar, 2019) and include mechanical exfoliation, laser-assisted, phase chemical/ electrochemical exfoliation, plasma-enhanced arc discharge, solvothermal, unzipping carbon nanotubes, liquid phase chemical or electrochemical exfoliation and unzipping of carbon nanotubes chemical vapour deposition and epitaxial growth (Kumar, 2019; Kumar, 2021). Chemical, thermal, microwave and laser reduction methods have been applied to prepare graphene from graphene oxide/graphite oxide.

* Corresponding author at: Department of Chemistry, Federal University of Technology, PMB 65, Bosso Campus, Minna, Nigeria.
E-mail address: oluwaseun_ajala81@yahoo.com (O.J. Ajala).

https://doi.org/10.1016/j.enmm.2022.100673
Received 24 June 2021; Received in revised form 6 February 2022; Accepted 1 March 2022
Available online 4 March 2022
2215-1532/

It should be noted that very few of these methods have been employed to obtain high quality and purity graphene. Besides, some other synthesis techniques have complex procedures, involving long chemical processes, and generate low quality amorphous graphene with structural defects and degradedness (Khan, 2016). Recent studies have identified chemical vapour deposition (CVD) technique as one of the very effective for the preparation of low-defect density and enhanced large area monolayer or film-layer graphene films through various kinds of precursor such as; gaseous, liquid, and solid precursor (Kumar, 2018; Kumar, 2017). On the contrary, CVD technique consumes time and uses large amounts of high purity gases and in addition demands high energy input. Plasma enhanced CVD utilized lower processing temperature however production of high quality graphene of enhanced surface area with less defects still remain a challenge. The choice of researchers to use different thermal and chemical methods to prepare large quantity of graphene flakes of different sizes and quality depend largely on the infrastructure availability and production cost.

More so, the non-existence of graphene alone except with graphite was abolished in 2004 when it was discovered that graphene can only exist separately through the use of scotch tape to separate graphite layers and obtain graphene crystals (Skoda, 2014). It was also opined that graphene cannot be decomposed due to thermodynamic instability since there is an existence of strong inter-atomic bonds between the carbon atom which prevented the crystal dislocation and defects (Yu, 2020). Due to these shortcomings of graphene, researchers have employed different strategy to improve the properties of graphene material through surface/structural modification, coupling with metal oxides or immobilisation with heteroatom depending on the mode of applications either as energy storage devices or as photocatalyst (Kumar, 2019). For instance, recent studies found improvement on the performance of energy storage devices when graphene derivatives and hybrids nanocomposites were modified with metal oxides/mixed metal oxides and metal sulfides/mixed metal sulphides.

In spite of widespread usage of graphene, it was demonstrated that graphene is not thermodynamically stable due to melting temperature which decreased with decreasing material thickness. Thus, oxidation of graphene to graphene oxide or graphene oxide based composite has been found to address the deficiencies of graphene alone (Li, 2018). GO contains oxygen functionalities (epoxy, hydroxyl, carboxyl and carbonyl groups) on its surfaces and edges which help in the attachment of metal oxide nanomaterials for energy-related applications. Graphene oxide (GO) can be easily synthesized in large scale via the chemical oxidation and exfoliation of graphite The efficiency vis-a-viz electronic structure and intrinsic properties of GO can be over tuned through chemical reactions at the interfaces, resulting in a material of high electrochemical performance (Kumar, 2019). GO based composite with graphene organic polymer has three categories of arrangement such as: organic functionalized graphene nanosheets; graphene-filled organic composites and layered graphene-organic films (Wang, 2019). The modification of graphene oxide based material through the introduction of reactive functional groups such as carboxyl groups among others have been found to enhance the photocatalytic and adsorptive properties of GO (Pandey, 2017). The presence of oxygen functionalities in graphene oxide allow easy dispersion in water and organic solvents, and the presence of different matrices are considered more advantageous for combination of Graphene oxide and ceramic or polymer matrices (Khan, 2016). In recent times, GO based nanomaterial has been employed as energy storage device and as photocatalyst modifier. For instance, several researchers have reported electrode potentials of GO. Kumar *et al.,* (Kumar, 2013), employed plasma-enhanced arc discharge method to produce high-quality thermally stable few-layer graphene (FLG) sheets (*4 layers) under argon atmosphere, using pure graphite rods as the electrodes with optimum Ar pressure of 500 Torr. Kumar *et al.,* (Kumar, 2017), provided recent progress on the laser-assisted synthesis of graphene and established the production of graphene of high quality and purity at low temperature and shorter reaction times. In the same vein, Kumar *et al.,* (Kumar, 2018), provided extensive review on recent advances on the synthesis and modification of carbon-based 2D materials for application in energy conversion and storage. Kumar *et al.,* (Kumar, 2019), provided information on the recent progress on the synthesis of graphene and derived materials for next generation electrodes of high performance lithium ion batteries and found that attachment of metal oxide/sulfide onto graphene improved its overall performance as anodes and cathodes for LIBs. Kumar *et al.,* (Kumar, 2020), summarised controlled synthetic approaches and heteroatom-doping mechanism strategy for various kinds of graphene-based materials for devices in energy-related applications using various chemical and physical routes. The authors found doping strategies suitable for tailoring the structure/properties of graphene materials in the area of energy applications. Kumar *et al.,* (Kumar, 2020), synthesised Mn_3O_4-Fe_2O_3/Fe_2O_3@rGO through simple and low cost microwave approach and the material was found to have specific surface area of 322 m_2/g with specific capacitance of 590.7F/g at 5 mV/s and cyclic stability as capacitance retention of 64.5 % after 1000 cycles at scan rate of 50 mV/s. Also, NiO/Co_2O_4 was synthesis by microwave approach and have surface area of 570 m^2/g which was very high due to high exfoliated GO nanostructure comprise of open edges (Kumar, 2020). A simple two-step microwave was used for the preparation of GO-Fe_2O_3 nanocomposites which resulted to 1693 and 1227 mAh/g of displayed discharge and charge capacities respectively. Hsu and Chen (Hsu and Chen, 2014) prepared reduced Graphene oxide-Ag nanocomposites through irradiation of microwave and was used as surface-improved Raman scattering substrate with high homogeneity and sensitivity. Kumar *et al.,* (Kumar, 2017); synthesized three dimensional (3D) reduced graphene oxide nanosheets (rGO NSs) containing iron oxide nanoparticles (Fe_3O_4 NPs) hybrids (3D Fe_3O_4/rGO) by one-pot microwave approach. They reported that the 3D hybrid materials has specific capacitances of 455F g^{-1} at the scan rate of 8 mV s^{-1}, which was superior to that of bare Fe_3O_4 NPs. Additionally, the 3D hybrid showed good cycling stability with a retention ratio of 91.4 after starting from ~190 cycles up to 9600 cycles. Kumar *et al.,* (Kumar, 2017), reported the controlled density of defects assisted perforated structure in reduced graphene oxide nanosheets-palladium hybrids for enhanced ethanol electro-oxidation and found that the synthesized hybrid material used as catalysts has improved sensitivity and current density of 10 mA/cm^2 for ethanol electro-oxidation. Kumar *et al.,* (Kumar, 2020), reported the synthesis of honeycomb-like open-edged reduced-graphene-oxide-enclosed transition metal oxides (TMO) (NiO/Co_3O_4) as improved electrode materials for high performance supercapacitor. It was established that the HOrGO/TMOs hybrids delivered high specific capacitance of 910F g^{-1} and high robust cycling stability with capacitance retention as 89.9% after continuous 2000 cycles than TMO (NiO/Co_3O_4) nanoparticles alone. Kumar et al., (Kumar, 2021), utilized microwave-assisted method to prepare hybrid thin reduced graphene oxide-cobalt oxide nanoparticles for electrode materials in supercapacitor and revealed that rGO@Co_3O_4/CoO hybrids electrode materials as supercapacitor showed specific capacitance of 276.1F g^{-1} (scan rate of 5 mV s^{-1}) and long-term cycling stability as 82.37% capacitance retention after 10,000 cycles (scan rate of 60 mV s^{-1}) in 0.1 M KOH electrolyte solution.

Furthermore, a review on heteroatom-doped graphene materials such as reduced graphene oxide, graphene oxide, graphene quantum dots and graphene nanoribbons in energy storage/conversion devices (supercapacitors, batteries, fuel cells, water splitting and solar cells have been reported. In spite of intense research efforts on GO, a review articles focused on the applications of hybrid graphene oxide based nanomaterials as photocatalyst and photo-fenton agent is rare. In view of this, the review provides insight on the properties, method of synthesis, and doping mechanism strategy of GO with heterogeneous semiconductor metal oxides, recent advances on graphene oxide based nanocomposites for the treatment of wastewater using photocatalytic, photo-Fenton and combination of photocatalysis and photo-fenton technologies.

2. Properties of graphene oxide

In this section, different properties of graphene oxide are discussed. This will help the reader to understand some important features of graphene oxide based nanostructured as an ideal material for photocatalytic technology. Graphene and graphene oxide often exhibit similar performance in water treatment. However, the synthesis of graphene oxide can easily be performed in large quantity compared to graphene or graphite and can be used as composites material, electronic, energy storage, biomedicine and biosensors to mentions but few. Some properties of graphene oxide are explained as follow (Khan, 2016).

2.1. Electrical properties

Graphene oxide usually has low electrical conductivity and poor thermal stability due to the disturbance of sp^2 bonds caused by the large defection and oxygen functionalities present. On the other hand, Loh *et al.,* (Loh, 2010) illustrated that graphene oxide exhibits excellent photo-luminescence which varies in wavelength from near-UV to near infrared. This becomes advantageous for bio-sensing and photo-electronics. The present of oxygen functionalities and defections has highly contributed to the chemical activity of GO which helps the reduction efficiency. Kashif *et al.,* (Kashif, 2021), compared electrical property of rGO and GO thin films and it was stated that the electrical property of reduced GO (6.32×10^{-4} A) was higher than the electrical properties of graphene oxide (6.86×10^{-7} A). This was attributed to the presence of low functional group of oxygen in the reduced graphene oxide. It was further established that the presence of many oxygen functional group in graphene oxide make it a suitable insulator material (Kashif, 2021).

2.2. Mechanical properties

Mechanical properties are referred to the mechanical characteristics of graphene oxide under different environments and various factors. These characteristics include Intrinsic Strength, Plasticity, Toughness, Hardness, Brittleness, Ductility, Rigidity, Elasticity, and Yield stress among others. Researchers have reported that the lowering of the energetic stability and breaking of sp^2 carbon network in graphene oxide contributed to decrease in the intrinsic strength and young's modulus monotonically which was further narrow its band gap under uniaxial tensile strain (Kashif, 2021). Gupta (Gupta, 2018), observed homogeneous stress distribution within graphene oxide with stiffness and strength of 40 GPa and 120 Mpa respectively. Xu *et al.,* (Xu, 2013), studied the use of wet spinning technique for production of GO fibres, where the dispersion of GO occurred in a liquid crystalline fibers and the coagulation bath were drawn via a rotating drum. Several of the articles on the study of the properties of mechanical of GO employed conventional mechanical measurement via tension to analyse the strength and modulus of the substance. However, Gómez-Navarro *et al.,* (Gómez-Navarro et al., 2008) employed Atomic Force Microscopy (AFM) for the examination of rGO sheets via deformation of tip-induced. The authors experimentally calculated the graphene oxide sheets Young's modulus to be 250 GPa (Robinson, 2008). Following this approach, Hu *et al.,* (Hu et al., 2010), also revealed graphene oxide (GO) Young's modulus with contact mode of finite element method (FEM) and atomic force microscopy (AFM) and to be 208 ± 23 GPa (Robinson, 2008). Several researchers have reported the characteristics, properties and formation of hybrid GO and GO (Xu, 2013) for application of aerogels (Xu, 2012), super capacitors (Zhao, 2015), stretchable conductor (Xu, 2013) and functional fabrics (Li, 2016) among others.

2.3. Thermal properties.

Thermal properties of GO are referred to its thermal conductivity associated with a material-dependent response when heated. This response may include a phase transition, a temperature increase, a change of volume or length, an initiation of reaction or the change of other chemical or physical quantities. Considering the thermal conductivity of synthesized graphene oxide using graphite as a precursor, Fang *et al.,* (Fang et al., 2016) reported low thermal conductivity of GO in the range of 0.5 – 1$Wm^{-1}K^{-1}$. This result was not ideal for good thermal properties application because Graphene is one of the highest in-plane thermal conductivities materials in the range of 3000 – 5000 $Wm^{-1}K^{-1}$, hence there is need to enhance the thermal conductivity of synthesised GO using polymer incorporated reduced GO. Fang *et al.,* (Fang et al., 2016), explained further that rGO films production through annealing of GO at high temperature of 1000 °C showed thermal conductivity from 3 to 61 $Wm^{-1}K^{-1}$ which is an improvement of in-plane thermal conductivity. Studies have proved that the incorporation of rGO into the polymers can lead to significant improvement of thermal conductivity property of material. Divya *et al.,* (Divya et al., 2019) incorporated poly (vinylidene fluorideco-hexafluoropropylene) into rGO and found that the synthesized nanocomposites had 19.5 $Wm^{-1}K^{-1}$ thermal conductivity which is of profound improvement over the thermal conductivity of graphene oxide. Apart from the rGO, there are many other factors that can enhance the thermal conductivity of GO. For instance, coupling of oxide of metal nanoparticle such as TiO_2, WO_3, ZnO with GO. Also, high orientation of the large sheet size that limited the thermal transfer along boundaries have been established to enhance the thermal property of reduced GO. Fig. 1 show the general method of synthesizing graphene oxide nanoparticles (Husnah, 2017).

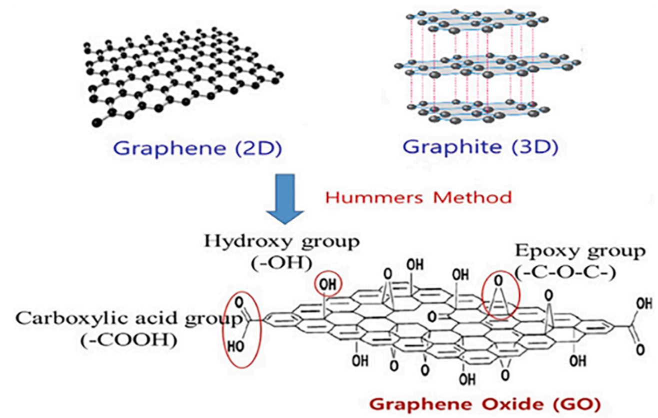

Fig. 1. General method of synthesizing graphene oxide nanoparticles (Husnah, 2017).

3. Mechanisms of graphene oxide based nanocomposites

In this section, three nanocomposites such as titania-graphene oxide, tungsten oxide – graphene oxide and iron oxide – graphene oxide are discussed. This will help the reader to understand the chemistry approach behind the application of these nanocomposites in photocatalytic performance. Graphene oxide based nanocomposites often exhibit similar performance in water treatment. The mechanisms are explained as follow;.

3.1. Mechanism of Titania-Graphene oxide based nanocomposites.

In water and wastewater treatment, Titanium dioxide photocatalyst has experienced continuous application due to its stability, high efficiency, and low cost (Prasad et al., 2020). However, it has some limitations such as large band gap energy with Anatase, Brookiite and Rutile, having the following band gap energy 3.2 eV, 3.4 eV, and 3.0 eV respectively. This makes it to only absorb UV light and as such exhibit recombination of photo-generated electrons and positive holes at fast rate (Kumar and Rao, 2017). Research data have shown that

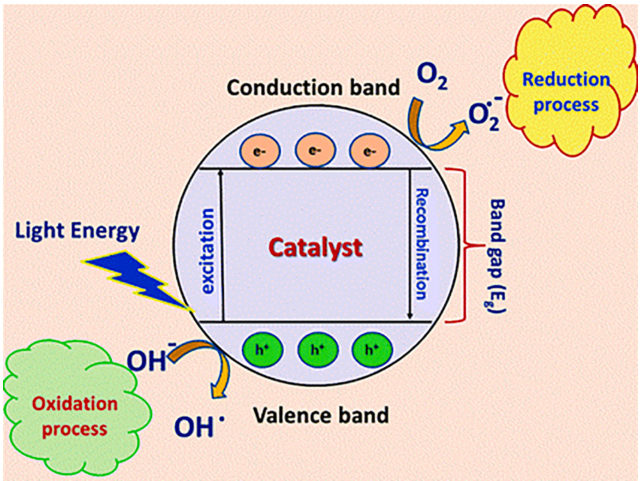

Fig. 2. Photoctalytic degradation mechanism of CV dye using TiO_2-GO nanocomposites under visible light (Saravanan et al., 2017).

incorporation of titanium oxide onto the lattice layer of graphene oxide would lower the recombination charge and the band gap energy of the two materials (Lingamdinne et al., 2019). The reduction of band gap energy was linked to the 2D profile of graphene oxide, which enables it to effectively separate the charges of TiO_2. Additionally, the unpaired p electrons of graphene oxide could fix with atom of Ti present in TiO_2 to generate Ti-O-C bonding which extend the range of absorption light of TiO_2. Under visible light radiation, studies have established that nanocomposites of Titania-graphene oxide possessed good photochemical responses which can be used in formation of H_2 in photon energy from decomposition of water (Sharma, 2018). Titania-graphene oxide based nanoarchitecture is made of shell - core such as shell of graphene oxide and core of TiO_2 which allowed close contact between the two components (Yuan, 2018). The electrons were extracted through the shell of Graphene oxide from the core of TiO_2 and evolved into evolution of H_2 from water under light irradiation (l > 320 nm). Sharma *et al.,* (Sharma, 2018), reported that the photosensitize crystal violet dye molecule absorbed visible light and produced a high state of energy from which a photoexcited electron was transferred into the conduction band of TiO_2 and then to GO. Due to the electron acceptor behaviour of GO having 2-D π-conjugation structure, the charge carriers recombination was suppressed. The oxygen react with these photo-excited electrons and form superoxide radical (O_2°) and thereafter, the valence band hole reacts with water and generates hydroxyl radical (OH°). These reactive oxygen species (OH° and O_2°) oxidized crystal violet to generate water, carbon dioxide, and intermediates. Ahmed *et al.,* (Ahmed, 2019), reported on the formation of GO-TiO_2 nanocomposite where GO was introduced onto TiO_2 lattice which enhanced the specific surface area, pore structure of the nanocomposites and prevent formation of agglomeration from TiO_2 nanoparticles. Furthermore, the authors reported that modification of Ti(IV) through GO in TiO_2 nanostructure increased the positively charged surface of the nanoparticles. It was also found that the composite material has fascinating optical properties. Joshi *et al.,* (Joshi et al., 2020) synthesised GO-TiO_2 nanocomposite for the mitigation of Rhodamine B and 94.59 % degradation efficiency was achieved after 120 min in the presence of electromagnetic radiation due to electron shift via band gap coupled with reactive oxygen species formation. The mechanism of degradation of crystal violet is expressed in equation (1) to (6) and Fig. 2 respectively:.

$$\mathrm{CV} + h\nu \rightarrow \mathrm{CV}\left(\mathrm{e_{CB}^-}\right) + \mathrm{CV}\left(\mathrm{h_{VB}^+}\right) \tag{1}$$

$$\mathrm{CV}\left(\mathrm{e_{CB}^-}\right) + \mathrm{TiO_2} \rightarrow \mathrm{TiO_2}\left(\mathrm{e_{CB}^-}\right) + \mathrm{TiO_2}\left(\mathrm{h_{VB}^+}\right) \tag{2}$$

$$\mathrm{TiO_2}\left(\mathrm{e_{CB}^-}\right) + \mathrm{GO} \rightarrow \mathrm{TiO_2} + \mathrm{GO}(\mathrm{e^-}) \tag{3}$$

$$GO(e^-) + O_2 \rightarrow GO + O_2^{\hat{A}^{o}-} \tag{4}$$

$$TiO_2\left(h_{VB}^+\right) + H_2O \rightarrow TiO_2 + OH\hat{A}^{o} \tag{5}$$

$$CV + O_2^{\hat{A}^{o}-} + OH\hat{A}^{o} \rightarrow CO_2 + H_2O + intermediates \tag{6}$$

3.2. *Mechanism of tungsten oxide - graphene oxide nanocomposites*

Tungsten oxide photocatalyst has experienced continuous application due to its narrow band gap (2.4 – 2.8 eV), low cost, thermostability, low toxicity, physicochemical stability, and high oxidative power (Isari, 2020). Tungsten oxide (WO_3) has been widely used as a visible light active photocatalyst which has several crystal forms, among which the monoclinic phase is known as the most stable form and exhibits the highest photocatalytic activity compared to others (Murillo-Sierra, 2021). Other forms of crystal are; tetragonal phase, orthorhombic phase and triclinic phase. Due to its narrow band gap, it is easy to absorb UV light and as such exhibit recombination of photo-generated electrons and positive holes at fast rate (Afify, 2019). The conduction band (CB) electrons in WO_3 are incapable of reducing dioxygen with a single electron transfer; surface modification approaches are required to efficiently separate photogenerated electrons and boost WO_3 photocatalytic activity (Basumatary, 2022).

Research data have shown that incorporation of tungsten oxide onto the lattice layer of graphene oxide would lower the recombination charge and the band gap energy of the two materials (Yadav et al., 2021). The oxidation of band gap energy was linked to the 2D profile of graphene oxide, which enables it to effectively separate the charges of WO_3 (Malefane, 2019). Additionally, the unpaired p electrons of graphene oxide could fix with atom of W present in WO_3 to generate W-O-C bonding which extend the range of absorption light of WO_3 (Zhao et al., 2020). Under visible light radiation, studies have established that nanocomposites of Tungsten oxide-graphene oxide revealed good photochemical responses which can be used in formation of H_2 in photon energy from decomposition of water (Marlinda, 2020). The mechanism of degradation of crystal violet is expressed in equation (7) to (12).

$$h\nu \rightarrow \mathrm{CV}\left(\mathrm{e_{CB}^-}\right) + \mathrm{CV}\left(\mathrm{h_{VB}^+}\right) \tag{7}$$

$$\mathrm{CV}\left(\mathrm{e_{CB}^-}\right) + \mathrm{WO_3} \rightarrow \mathrm{WO_3}\left(\mathrm{e_{CB}^-}\right) + \mathrm{WO_3}\left(\mathrm{h_{VB}^+}\right) \tag{8}$$

$$\mathrm{WO_3}\left(\mathrm{e_{CB}^-}\right) + \mathrm{GO} \rightarrow \mathrm{WO_3} + \mathrm{GO}(\mathrm{e^-}) \tag{9}$$

$$GO(e^-) + O_2 \rightarrow GO + O_2^{\hat{A}^{o}-} \tag{10}$$

$$WO_3\left(h_{VB}^+\right) + H_2O \rightarrow WO_3 + OH\hat{A}^{o} \tag{11}$$

$$CV + O_2^{\hat{A}^{o}-} + OH\hat{A}^{o} \rightarrow CO_2 + H_2O + intermediates \tag{12}$$

3.3. *Mechanism of iron oxide-Graphene oxide Nanocomposites.*

According to Equations (13) and (14), the reaction takes place primarily at the solid–liquid interface, where the active sites (Fe^{2+}/Fe^{3+}) of Fe_3O_4 NPs attached to the surface of GO sheets catalytically breakdown the adsorbed H_2O_2 into $HO^{\bullet}$ radicals and hydroperoxyl radicals ($HOO^{\bullet}$). H_2O_2 was also activated and degraded on the GO surfaces to create $HO^{\bullet}$ radicals, in addition to the Fe_3O_4 active sites (Geraldino, 2020). The intrinsic donor–acceptor surface features of carbon materials are attributed to this phenomena via an electron transfer reaction (Song, 2020) similar to the photo-Fenton mechanism, with $GO_{C=C,\ sp2}$ and $GO_{C\text{-}C,\ sp3}$ being the reduced and oxidized carbon active sites, respectively (Equation (15) and (16)).

Furthermore, the existence of numerous semiconducting conjugated sp2 carbon domains on GO's basal planes results in unpaired electrons,

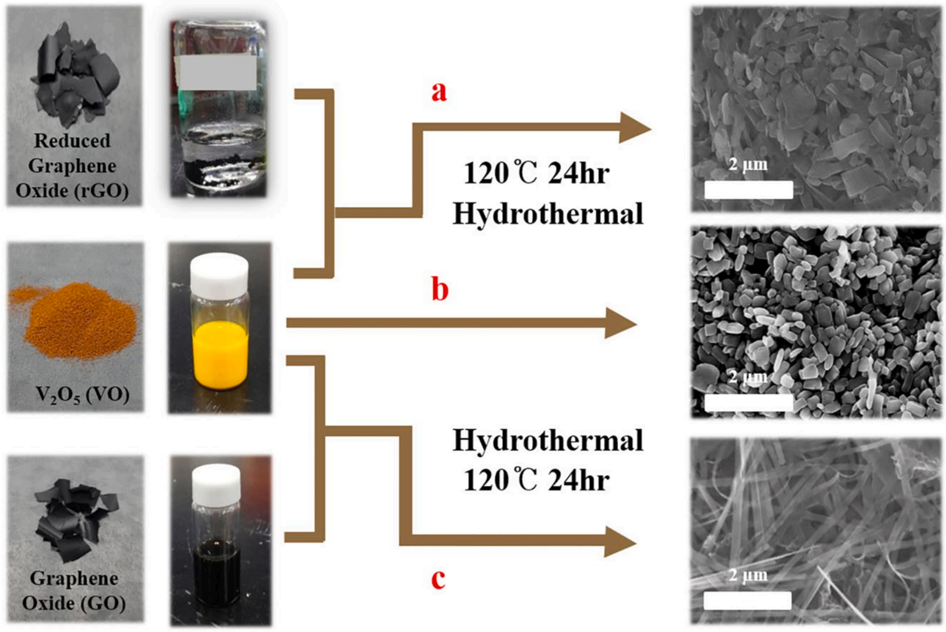

Fig. 3. Synthesis of Graphene oxide based Nanocomposites using Hydrothermal Method (Lee, 2015).

which can enable electron transfer between GO and iron centers via Fe–O–C bonds (Zhuang, 2019). This electron transfer could be linked to the GO (–0.19 V) reduction potential vs. saturated calomel electrode (SCE), which is lower than the usual Fe^{3+}/Fe^{2+} reduction potential (+0.771 V) (Li, 2020). The electron may be given from the GO basal planes to the oxidized active sites, spontaneous reduction of Fe^{3+} to Fe^{2+} was feasible (Morant Giner, 2020). Since, the reduction of Fe^{3+} by H_2O_2 to Fe^{2+} was relatively slow, such synergistic interaction between the GO and Fe_3O_4 NPs is beneficial in accelerating the Fe^{3+}/Fe^{2+} redox cycles (Equation (17)) for the fast reduction of Fe^{3+} to Fe^{2+}, which is actively participating in the decomposition of adsorbed H_2O_2 into HO• radicals during catalysis (Morant Giner, 2020). As a result, the efficient cyclical electron transfer between GO and Fe_3O_4 NPs in GO–Fe_3O_4 nanocomposites plays a key role in the modification of the surface redox processes that allowed for high pollutants elimination in the heterogeneous photo-Fenton reaction.

$$Cv + hv \rightarrow Cv\left(e_{CB}^{-}\right) + Cv\left(h_{VB}^{+}\right) \tag{13}$$

$$Fe^{2+} + H_2O_2 \rightarrow Fe^{3+} + OH^{\cdot} + OH^{-} \tag{14}$$

$$Fe^{3+} + H_2O_2 \rightarrow Fe^{2+} + HOO^{\cdot} + H^{+} \tag{15}$$

$$GO_{C-C,sp3} + H_2O_2 \rightarrow GO_{C=C,sp2} + HOO^{\cdot} + H^{+} \tag{16}$$

$$GO_{C=C,sp2} + Fe^{3+} \rightarrow GO_{C-C,sp3} + Fe^{2+} \tag{17}$$

4. Methods of synthesizing graphene oxide nanostructured material

In this section, different approaches for the synthesis of GO nanostructured materials were explained. This will help to give an insight on importance and comparative merit of one method over the other methods.

4.1. Hydrothermal method

This is a technique used for the synthesis of nanoparticles through an aqueous media at high pressure and temperature. Several researchers have investigated the application of hydrothermal technique for the preparation of GO nanostructured material (Lingamdinne et al., 2019). The precursors of hydrothermal technique are organic molecules in the alkaline media. Although, hydrothermal technique is considered economical and eco-friendly, it usually involves high temperature (Jose, 2018). The temperature range between 160 and 180 °C in an autoclave (Jose, 2018). However, there are some limitations such as; inability to monitor the growth of the crystal material in the autoclave and the cost of the equipment. Nawaz *et al.,* (Nawaz, 2017), evaluated the synthesis of rGO-TiO_2 using hydrothermal method for photo-degradation of carbamazepine. It was observed that the nanostructured material (rGO-TiO_2) exhibited high rate of adsorption and photo-degradation than TiO_2 as>99 % carbamazepine removal was achieved within 90 min (Adeyanju, 2022). This was attributed to the effectiveness of rGO during the preparation of rGO-TiO_2. Zhang *et al.,* (Zhang, 2020), also carried out study on synthesis of CuO-Cu_2O/GO nanocomposites using hydrothermal method for degradation of tetracycline and organic dye. It was reported that the designed nanocomposite have excellent dual function for catalytic oxidation of methyl orange with 95 % degradation and tetracycline with 90 % degradation after 120 min. Pant *et al.,* (Pant et al., 2020) evaluated the preparation of Ag_2CO_3-TiO_2 nanomaterial through hydrothermal technique at 130 °C for 4 h and found that adsorptivity enhanced charge separation, transportation properties and extend photo-responding range among others. It was further revealed that the photocatalytic degradation of Methylene blue dye and the nanocomposites restrained the recombination rate of photo-generated electron-hole pairs and greatly extends the lifetime of charge carriers. Fig. 3 summarized hydrothermal synthesis method of graphene oxide based nanocomposites.

4.2. Solvothermal method

This technique is used for preparation of different nanoparticles via non-aqueous media at high pressure and temperature. Solvothermal technique can be classified into two categories such as; synthesis in the media of alkaline media and in the presence of precursors of organic molecules (Yuan, 2021). This route of synthesis is considered innovative, because few published papers on the production of graphene oxide were found in the literature. Solvothermal approach for producing graphene oxide has several advantages such as; non-toxic, cost effectiveness, and with almost no by-products in the process of the reaction

Fig. 4. Synthesis of Graphene oxide based Nanocomposites using Solvothermal Method (Yadav and Kim, 2016).

(Chin, 2019). For instance, Yuan *et al.,* (Yuan et al., 2012) investigated the fabrication of graphene-Ag nanocomposites through deposition of synthesized silver on graphene using solvothermal techniques. The authors established an excellent electro-conductibility through deionized water/hydrazine or ethylene glycol. The size and morphology of silver nanoparticle was controlled by hydrazine used as a reducing agent. Lin-jun *et al.,* (Lin-jun 2012), also employed solvothermal technique to synthesise graphene-Ag nanocomposites and found that the composite material have electro-conductibility of 2.94 scm^{-1}. Lin-jun *et al.,* (Lin-jun 2012) synthesized graphene-Mn_3O_4 nanocomposites through solvothermal method in ethanol solution and it was reported that the grown material is a potential material for super-capacitor with the mass percent of Mn^{2+} and graphene oxide as 10 and 90 respectively which also revealed capacitance with high specific of ~245F/g at 5 mV/s. Yuan *et al.,* (Yuan, 2021) also developed three dimensional graphene-CoO nanocomposites through solvothermal route with enhanced electrochemical performance as lithium battery. Generally, combination of ultra and sono-chemical method was applied to develop the dispersion and prevent re-aggregation. Fig. 4 summarized solvothermal synthesis method of graphene oxide based nanocomposites.

4.3. Co-precipitation method

This involves co-precipitation of metal cations from oxalates, carbonates, formats or citrates, hydroxides among others (Pu, 2018). These precipitates are converted into powders at suitable temperatures. This method has shortcoming such as presence of undesirable impurities which also co-precipitate with the analyte (Pu, 2018). This shortcoming can be alleviated by re-precipitating the analyte which bring about inclusion (when contaminant causes a frame site in the crystal structure of the transporter which is about a fault crystallographic) and occlusion (when an adsorbed contamination becomes physically surrounded inside the crystal). Many nanocomposites have been synthesized using co-precipitation method such as; CeO_2-ZnO-$ZnAl_2O_4$ and even among graphene oxide based nanocomposites. Ranjith *et al.,* (Ranjith, 2019), evaluated the photocatalytic efficiency of rGO-TiO_2/Co_3O_4 nanocomposites prepared through co-precipitation technique on dyes. The synthesized materials were characterized using field emission scanning electron microscopy (FESEM) and the analysis revealed the existence of TiO_2/Co_3O_4 adsorbed on rGO surface while UV–visible spectrophotometer (UV–vis) and the spectra of photoluminescence (PL) showed that emission and absorbance occurred at visible regions which support the degradation process via the separation of the electron-hole. The rGO-TiO_2/Co_3O showed highest degradation performance of dyes under visible light irradiation. However, this requires improvement through combination of methods such as co-precipitation and intercalation polymerization techniques. For instance, Mu *et al.,* (Mu, 2017), investigated magnetic graphene/polyaniline nanocomposites prepared via in

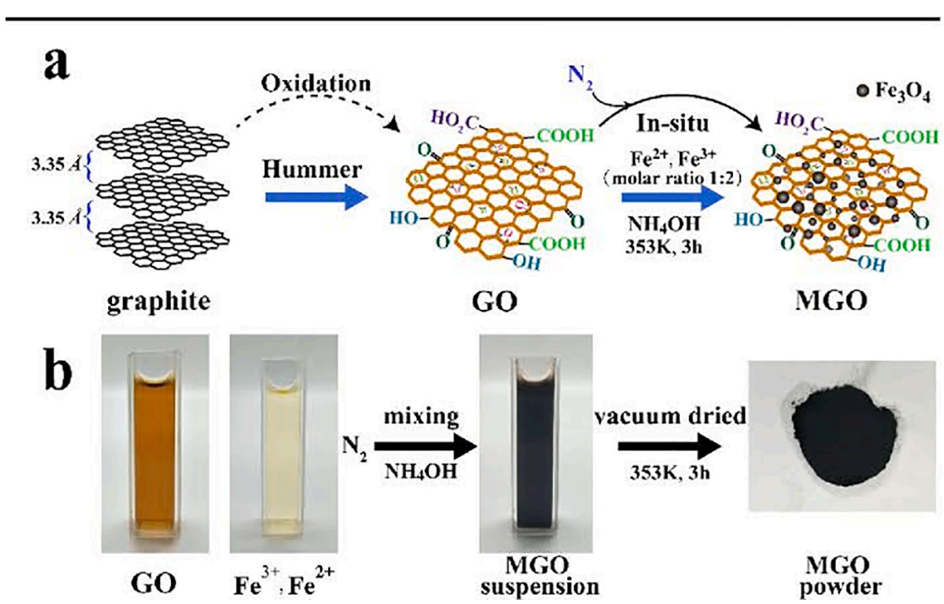

Fig. 5. Synthesis of Graphene oxide based Nanocomposites using Co-precipitation Method (Pu, 2018).

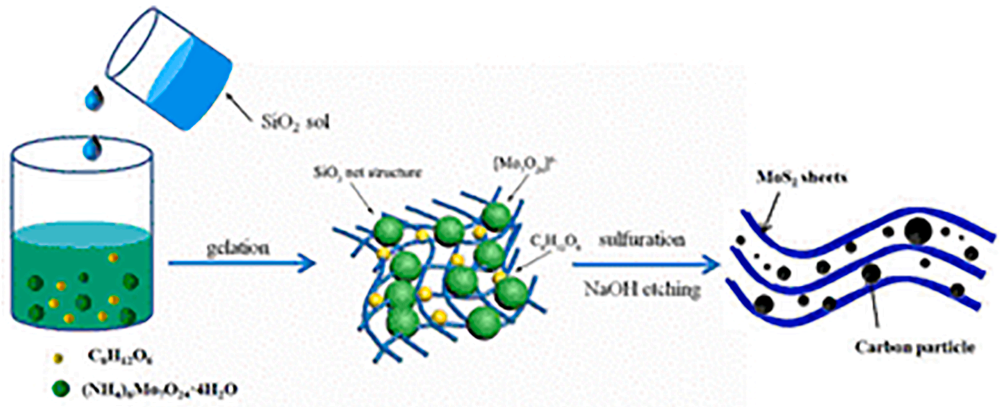

Fig. 6. Synthesis of Graphene oxide based Nanocomposites using Sol-gel Method (Guo, 2018).

situ or one pot co-precipitation and intercalation polymerization technique and applied the material for the degradation of dyes. Chinnathambi and Alahmadi (Chinnathambi and Alahmadi, 2021), reported the synthesis of Fe_3O_4 /polyaniline/GO through the combination of processes of intercalation polymerization and co-precipitation techniques. Its adsorption capacity was found to have high presence of anionic ions such as phosphate ions through selectivity and recyclability tests from wastewater. It was illustrated through Fig. 5.

4.4. Sol-gel method

This is a simple and inexpensive wet-chemical method used in the preparation of composite materials of an excellent control size. In this technique, the solution (sol) evolves gradually towards the production of a gel - like formation which consists of solid and liquid phase. There are two categories of sol–gel techniques which are aqueous and non-aqueous sol–gel synthesis. In non-aqueous sol–gel preparation of metal oxide nanoparticles, the first step towards development of rational synthesis is elaboration of chemical formation mechanism along with the studies on the crystallization process However, to ensure

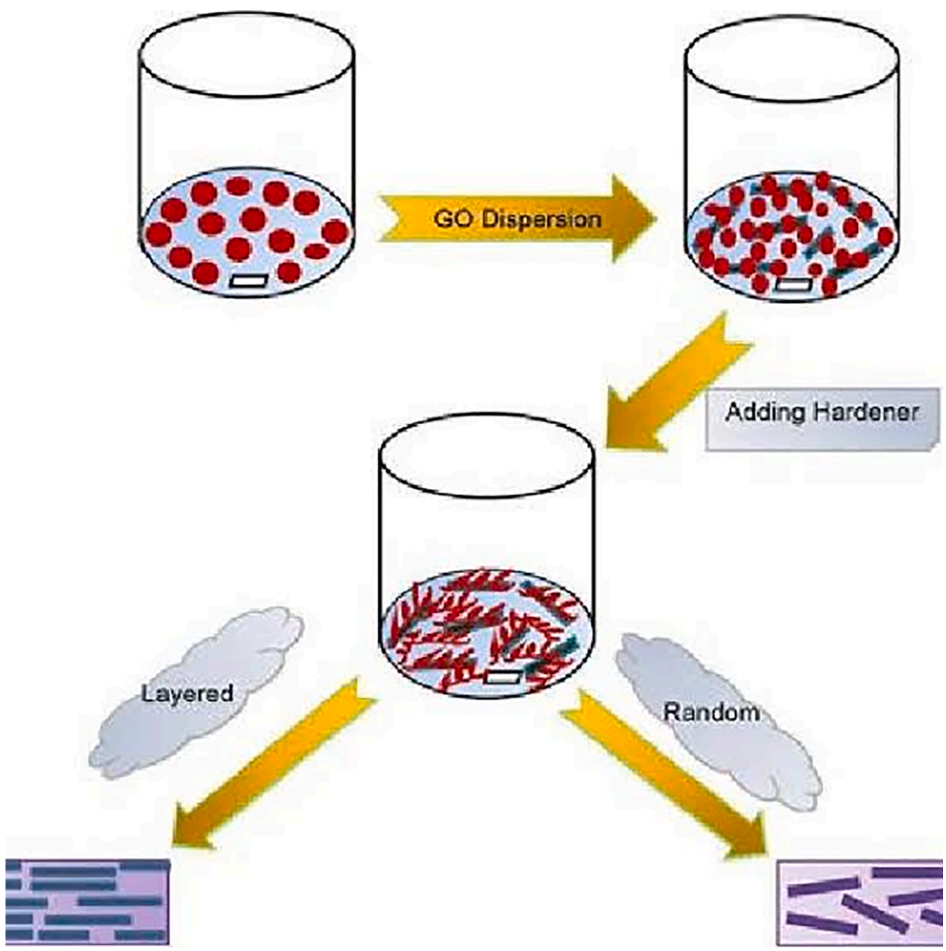

Fig. 7. Synthesis of Graphene oxide based Nanocomposites using **Solution Mixing Method** (Kausar, 2016).

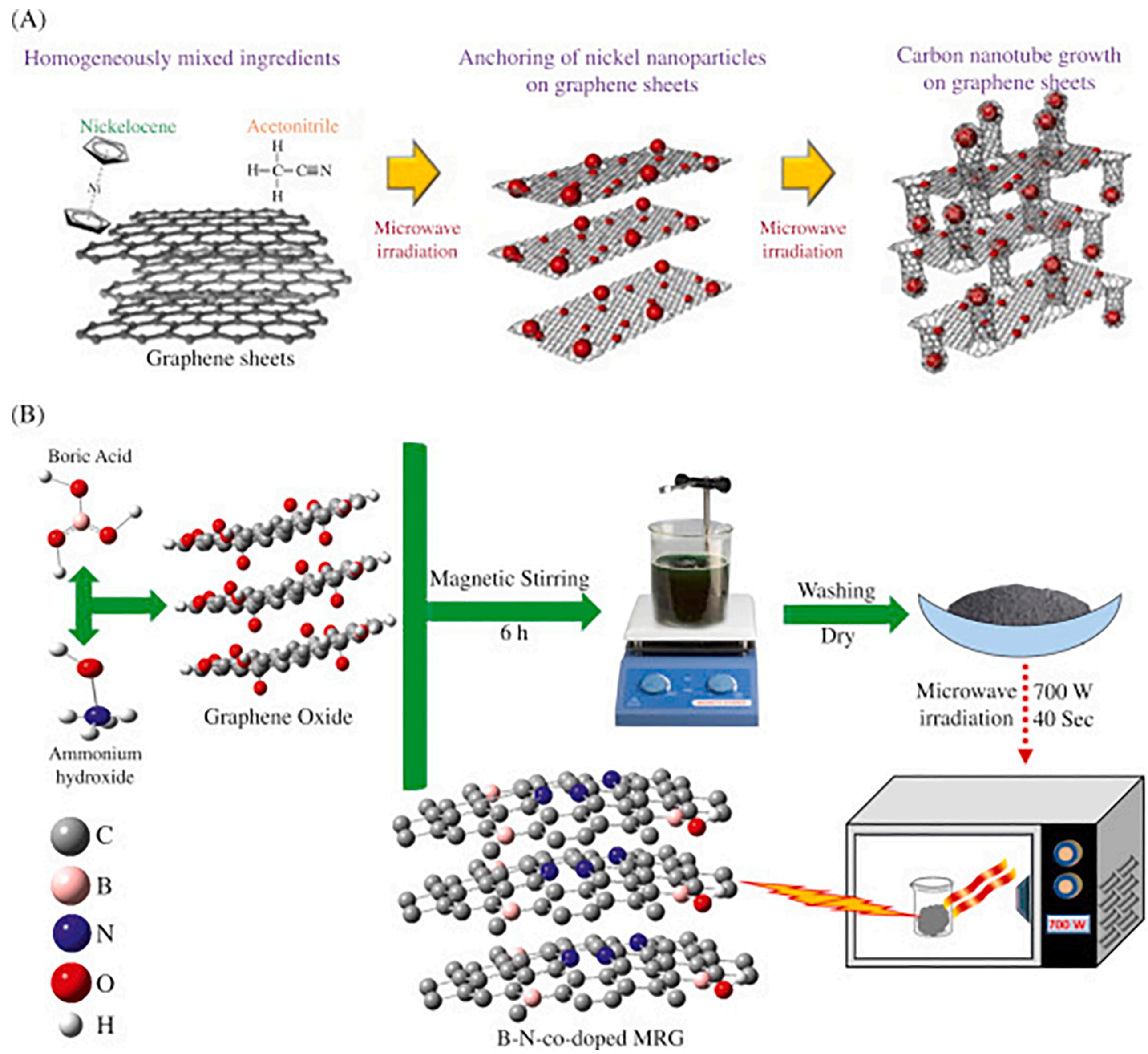

Fig. 8. Synthesis of Graphene oxide based Nanocomposites using Microwave irradiation Method (Seekaew, 2019).

comprehensive result of this technique, there is need to investigate different characterizations properties such as; microscopy and crystallographic among others. It has been discovered that this method makes the study of organic species transformation in the reaction mixture easy through standard techniques such as: Nuclear Magnetic Resonance (NMR) and Gas Chromatography-Mass spectrometry (GC–MS) among others.

In contrast, hydrolysis of metal alkoxides rate is fast in aqueous media of sol–gel method which complicates the control rate of reactions. In non-aqueous sol–gel method, the application of moderate reactivity of the carbon–oxygen bond is possible at low reaction temperature and this makes the nanoparticle to exhibit high crystallinity. Although, there are different reports on non-aqueous procedures in the synthesis of metal oxide nanoparticles (Lee et al., 2017), the organic reactions can be classified into seven mechanisms; (1) thermal decomposition, (2) alkyl halide elimination, (4) oxidation of metal nanoparticles, (5) ether formation, (6) ketimine and aldo-like condensation and (7) C–C bond formation. There are three different categories of organic solvents applied in non-aqueous sol–gel reactions: (i) non-reacting or inert solvents such as mesitylene or toluene, (ii) oxygen-containing solvents like ketones or aldehydes, alcohols, and (iii) other reactive functional group with oxygen-free solvents such as amines or nitriles. The appropriate choice of the solvent is essential, because mechanism formation of the nanoparticles is highly influence. For instance, Ma *et al.,* (Ma, 2018), applied GO and tetrabutyl titanate as the precursor to synthesis GO-TiO_2 nanocomposites and revealed that the activity of photocatalytic of the composite was influenced by both the content of graphene oxide and the atmosphere of calcinations. Ultra-disperse titania nanoparticle on graphene was synthesised using sol–gel and achieved the specific capacity twice as that of mechanical mixed composite (Pan, 2020). Fabrication of controlled carbon phase based rGO-SiO_2 via sol–gel technique improved the conductivity capacity of the composites compared to SiO_2 alone (Sengupta, 1911). Fig. 6 summarized sol–gel synthesis method of graphene oxide based nanocomposites.

4.5. Solution mixing method

This is a widely applied technique in the synthesis of GO/metal oxide nanomaterials due to its low temperature, fast de-aggregation and uniform reinforcement dispersion of the produced composite. The basic of solution mixing technique is in a solvent system. This technique involves mixing of two different nanoparticles in a solution via electrospinning.

Table 1
A brief summary of research studies on the methods of preparation of graphene oxide based nanocomposites.

Method	Nanocomposites	Synthesis conditions or Parameters varied	Significant findings	Research Gap	References
Microwave irradiation	CuS-reduced graphene oxide	Ultrasonication for about 2 h, at room temperature, magnetic stirring for 1 h, microwave irradiation at 120 °C for 30 min, precursors: 50 mL of GO (1 mg/mL) and 25 mL of $CuSO_4 \cdot 5H_2O$ solution (10 mM).	The synthesized nanocomposite was efficient photocatalyst for the degradation of diazo congo red molecule under natural sun light irradiation. the degradation efficiency is 98.76 % compare to the 88.98% of TiO_2 only.	The study revealed that effect of stirring speed, time and solution pH was not investigated on the particle size formed	(Borthakur, 2016)
Solvothermal	TiO_2-graphene oxide	Sonication: 30 min, Teflon-lined autocave at 130 °C, 4 h Precursors: 1.0 g anatase TiO_2 and graphite powder.	TiO_2-GO exhibited better photocatalytic performance than pure TiO_2 nanoparticles.	The band gap energy was not study. Green synthesis was not employed in the synthesis of TiO_2 and GO nanoparticles.	(Yadav and Kim, 2016)
Hydrothermal	TiO_2/RGO	1 h, 170 °C, pH 7, under a constant N_2 flow for 2 h. precursors: 1.0 g natural graphite, 2.8 mmol of sodium dodecyl benzene sulfonate, 2.8 mmol Triton X-100 and 2.8 mmol cetyl trimethyl ammonium bromide.	- TiO_2/RGO exhibited a significant photocatalytic efficiency on Methylene blue with 97.5 % in 120 min.	-The authors did not optimize the synthesis parameters.	(Hu, 2017)
Co-precipitation	Graphene oxide/Fe_3O_4	-Under N_2 atmosphere. - Low pH (pH = 1.89) to prevent aggregation, the pH was adjusted. − 333.15 K -vacuum conditions −8h. Precursors: 2.0 g graphite powder, 1.2 g sodium nitrate, 1.3 mmol $FeCl_2 \cdot 4H_2O$ and 2.6 mmol $FeCl_3 \cdot 6H_2O$.	The Nanocomposite showed a high adsorption efficiency relevant to the purification of dye-contaminated wastewater and readily separated due to its magnetic behaviour. The maximum adsorption capacity was 546.45 mgg^{-1} for the methylene blue and 628.93 mgg^{-1} for the Congo red.	- No optimization of synthesis parameters such as reaction time, stirring speed, solution pH among others.	(Pu, 2018)
Sol –gel	TiO-rGO-Fe_2O_3	Sonication: 1 h, autocave at 180 °C for 10 h, dried for 60 °C for 12 h, precursors: graphite powder of 5 g, 140 mL H_2SO_4 $NaNO_3$ of 2.5 g, 683 mg of $FeCl_3$ and 584 mg of $FeSO_4$.	99% removal of the dye within 6 min under irradiation of UV, 94 % was removed under visible light.	-The synthesized nanoparticles were not synthesis using green synthesis. The photocatalytic activity was not studied under ultraviolet light.	(Banerjee, 2018)
Sol- gel	GO-TiO_2	Sonication: 45 min, Annealing at 450 °C, precursors: 1 g of titanium dioxide, 1 g of graphite.	The Photocatalytic activity showed a significant increment with the addition of GO. The film exhibited potential application in the photoreduction of CO_2.	There was no optimization study on reaction time, stirring speed on the particle.	(Hernández-Majalca, 2019)
Co-precipitation	GO-ZrO_2	Ultrasonication 30 min, Sonication: 30 min, maintaining the pH above 10.5 under stirring. Precursor: 1 mmol zirconium oxychloride salt, 0.5 g of GO.	90 % and 99.23 % photocatalytic degradation of Rhodamine B dye and Methylene blue was observed in 105 min and 60 min respectively.	Real effluent was not use in degradation analysis.	(Das, 2019)
Solution mixing	GO/Polyacrylamide	90 °C, 2 h for stirring. Precursors: 25 mg of GO, 25 μL hydrazine hydrate solution, 5 mg Polyacrylamide.	The GO/PAM membrane has the best comprehensive separation performance since its proper interlayer spacing.	The band gap energy was not investigated and different light source was not investigated on photocatalytic activities	(Cheng, 2019)
Solution mixing	RGO/acrylonitrile butadiene styrene (ABS)	Thermally exfoliation of GO in a microwave oven, sonication in ethanol, solution mixing inside ball mill for 6 h. precursors: graphite oxide and 6-amino-4-hydroxy-2-naphthalenesulfonic acid	61 % increment in elastic modulus compared to ABS. better interaction with ABS matrix which improved the mechanical properties of the composites	The study revealed that effect of stirring speed, time and solution pH was not investigated on the particle size formed	(Mustapha et al., 2019)

However, the major drawback is the potential leaching of the additional material since no chemical bonding between added material and the base. For instance, Suneetha *et al.,* (Suneetha et al., 2019) investigated the preparation of ternary nanocomposites of Zinc doped Iron oxide/GO/Polymer by solution mixing technique. The impedance analysis revealed that the nanocomposites modified electrode have good capacitance with bode phase angle 87° and considered a good candidate for super capacitor application. In addition, Zeng *et al.,* (Zeng, 2018) synthesized Al-graphene oxide composites using ultrasonic techniques and the authors found that the graphene oxide-Al nanocomposites had 255 MPa tensile strength. It has been proved that fabrication of graphene oxide metal oxide/metal nanocomposites have enhanced mechanical properties and also addressed different energy and environmental related issues. Also, Nawaz *et al.,* (Nawaz, 2018) evaluated efficient way for the preparation of graphene-TiO_2 nanomaterials through UV-assisted photocatalytic reduction of graphene oxide in solution phase. Galpaya *et al.,* (Galpaya, 2014), fabricated epoxy nanocomposites with graphene oxide loading via solution mixing and found that the small quantities of graphene oxide incorporated into the epoxy matrix contributed significantly to epoxy mechanical properties. The authors further explained that the elastic modulus increase steady with the addition of graphene oxide from 0.1 wt% to 0.5 wt% whereas there was no significant effect on graphene oxide incorporated on tensile strength. Prabhu *et al.,* (Prabhu, 2019), utilized solution mixing technique for the fabrication of ZnO Dumbbell/rGO nanocomposites used for degradation of methylene blue and methyl orange under the irradiation of UV–Visible light. The data showed that ZnO/rGO nanostrutured materials have higher degradation efficiency than rGO and ZnO dumbbell. Fig. 7 summarized solution mixing synthesis method of graphene oxide based nanocomposites.

4.6. Microwave irradiation method

Another method used for the synthesis of inorganic nanomaterials is microwave irradiation method which does not consume much energy. It is environmental friendly, fast and generates homogenous heating process (Afzal et al., 2018). Microwave radiation technique offers several advantages such as reduction in time of reaction to generate cleaner reaction environment with energy saving through rapid and intense heating in the interior of the sample (Afzal et al., 2018). Researchers have applied microwave method to generate several graphene oxide based nanocomposites to mention but few; rGO-$Ni_{0.4}Zn_{0.4}Co_{0.2}Fe_2O_4$ nanocomposites (Liu et al., 2015) and Mn_3O_4-rGO nanocomposites (Varghese, 2019) among others. In the study of Liu *et al.,* (Liu et al., 2015), the authors investigated that the prepared nanocomposites exhibited an excellent broad absorption bandwidths and electromagnetic wave absorption properties compared with rGO and $Ni_{0.4}Zn_{0.4}Co_{0.2}Fe_2O_4$. The authors failed to use the prepared nanocomposites for any degradation process. Varghese *et al.,* (Varghese, 2019), also reported that graphene oxide based electrode exhibits enhanced electrochemical properties. Though most graphene oxide based nanocomposites are prepared using hydrothermal method due to its ecological friendly and economic feasibility even at high temperature and pressure (Lingamdinne et al., 2019). There are also few studies which combined hydrothermal method with microwave or ultrasonic-sonochemical method. The fabrication of graphene oxide based nanocomposites via irradiation of microwave was done in multiple cycles to subside overheating. The dispersion of precursor was done inside ultra-sonication with stirring in period of time (Chook, 2012). The slurry was preserved in a microwave employing multiple cycle followed by filtration and moisture removal from the product (Chook, 2012). A simple two-step microwave was used for the preparation of GO-Fe_2O_3 nanocomposites which resulted to 1693 and 1227 mAh/g of displayed discharge and charge capacities respectively. Hsu and Chen (Hsu and Chen, 2014), prepared rGraphene oxide-Ag nanocomposites through irradiation of microwave and was used as surface-improved Raman scattering substrate with high homogeneity and sensitivity. Fig. 8 summarized microwave irradiation synthesis method of graphene oxide based nanocomposites. Table 1 summarized different studies with different methods used in the fabrication of GO based nanocomposites.

From table 1, microwave irradiation, solvothermal, hydrothermal, co-precipitation, sol–gel, and solution mixing have been used to prepare GO based nanocomposites. It was found that all the methods were suitable and effective for the synthesis of high yield graphene oxide based nanocomposites however there is no any approach without different advantages and disadvantages. Therefore, it is advisable to choose suitable approach based on the availability of materials, equipment and production of desire products. There are many aspects untouched in those literatures such as optimization of parameters, investigation of band gap and their application to real environmental samples for pollutant removal.

5. Structural characterization and properties of graphene oxide based Nanocomposites.

The formation of GO nanostructured materials can be evaluated by the following spectroscopic techniques; X – Ray Photoelectron Spectroscopy (XPS), X-Ray Diffraction (XRD) and Fourier Transform Infrared (FT-IR) for the identification of chemical composition, structure, formation, crystalline phase and functional group respectively. The

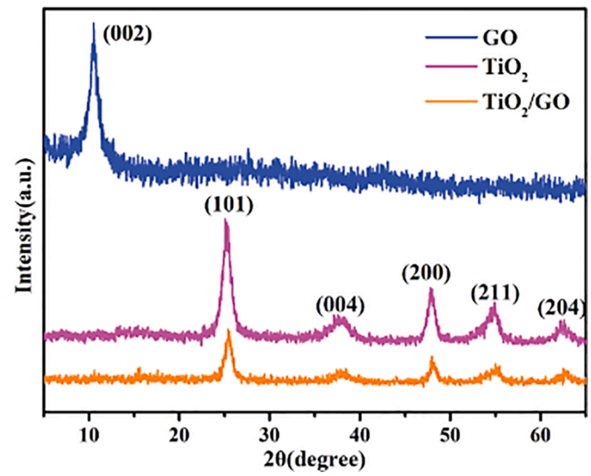

Fig. 9. XRD Pattern of GO, TiO_2 and TiO_2/GO Nanocomposites (Zhang, 2018).

porosity, size and surface morphology can be characterized via microscopic techniques namely; High Resolution Scanning Electron Microscope (HRSEM) and High Resolution Transmission Electron Microscope (HRTEM). Brunauer-Emmett-Teller (BET) N_2 adsorption–desorption while magnetometer is used to determine the magnetic property of the nanocomposites. Thermagravimetry analysis (TGA) and Raman spectroscopy were used to determine the thermal stability profile and molecular bonding in GO based nanocomposites.

5.1. XRD analysis of graphene oxide based nanocomposites

XRD analysis is majorly used for the identification of the chemical structure, formation of any possible phase and nature of the of graphene oxide nanocomposites. XRD patterns have shown that strong diffraction peaks at (2θ) values from 8° to 12° confirming the presence of Graphene oxide (Vajedi and Dehghani, 2016). When ferrites was coupled with graphene oxide to form nanocomposites, the size of the graphene oxide based nanocomposites decreases, the porosity increases; thus, the diffraction peaks position shifted to lower diffraction angle (Lingamdinne, 2016). Over the years, ferrites peaks have been detected in graphene oxide based nanocomposites through XRD analysis. Shan *et al.,* (Shan, 2017) found that the diffraction peaks of GO nanoparticle was located at 2 thetha value of 10.6° while diffraction peaks belonging to graphene oxide-goethite based nanocomposites were located at 2 thetha values of 20.92°, 32.66°, 35.96° and 53.06° which correspond to goethite. This shows that goethite crystal structure did not change after modification with graphene oxide. However, there was no peak at 10.6° for graphene oxide and the disappearance indicates reduction of graphene oxide during synthesis. The graphene oxide-goethite based nanocomposites was utilized for the degradation of tylosin pollutant and 84 % degradation efficiency was achieved compared to 47 % degradation efficiency of graphene oxide nanoparticle in the presence of simulated sun light irradiation at 120 min. From different studies, it was observed that doping and coupling of graphene oxide nanoparticle goethite always resulted to higher degradation efficiency of organic pollutants in wastewater. Zhang *et al.,* (Zhang, 2018), also reported the pattern of XRD for TiO_2, GO and TiO_2/GO nanocomposite shown in Fig. 9. There was successful oxidation of graphite to GO due to the strong peak at 2θ of 10.54° which correspond to (0 0 2) crystal plane. Also, the theoretical value of interlayer spacing of GO powder (0.34 nm) was lower than the experimental GO powder (0.84 nm) due to the presence of oxygen functional group. For TiO_2, the following diffraction peaks were found at 2θ values of 62.63°, 54.98°, 47.99°, 37.77°, and 25.28° with the following crystal planes (2 0 4), (2 1 1), (2 0 0), (0 0 4) and (1 0 1) depicting anatase types of TiO_2 while the diffraction peaks of TiO_2/GO nanocomposites were similar with that of TiO_2 and can be attributed to

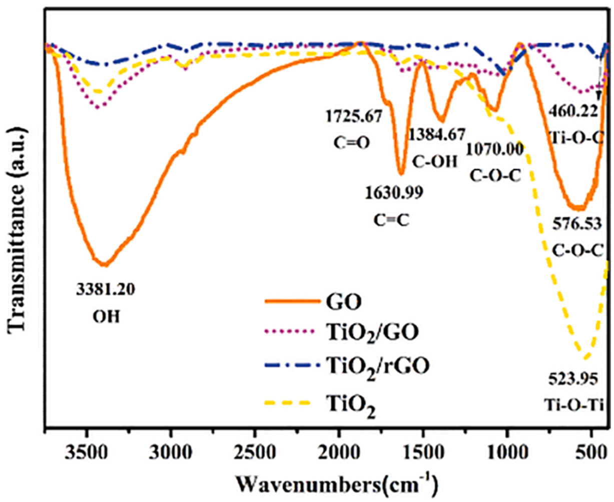

Fig. 10. FTIR Spectra of TiO_2, GO, TiO_2/rGO and TiO_2/GO and nanostructured materials (Zhang, 2018).

the destruction of the regular stack of GO sheet through intercalation of TiO_2 nanoparticles. This was illustrated in Fig. 9.

5.2. Magnetometer analysis of graphene oxide based nanocomposites

Graphene oxide has a magnetic characteristic that can be evaluated via the magnetic measurement system. When there is a reduction in size of graphene oxide based nanocomposites to nano-scale, the material usually exhibited super-paramagnetic behaviour (He, 2018). The super-paramagnetic property of GO based nanomaterials can be explained using magnetization vs. temperature (MT) curves since it is temperature dependent. For instance, Lingamdinne *et al.,* (Lingamdinne, 2017) obtained magnetic field of 1000 Oe and the super paramagnetic nanocomposites MT curves, field cooled and zero-field cooled curves were found to increase linearly with decrease in temperature. It was reported that nickel ferrite nanocomposites were super-paramagnetic at room temperature (Nejati and Zabihi, 2012). In magnetization, the presence of mesoporous carbonaceous material decreased the graphene oxide crystalline property due to the alternation of the original GO peak (Vajedi and Dehghani, 2016). When ferrite was coupled with graphene oxide to form nanocomposites, the size of the graphene oxide based

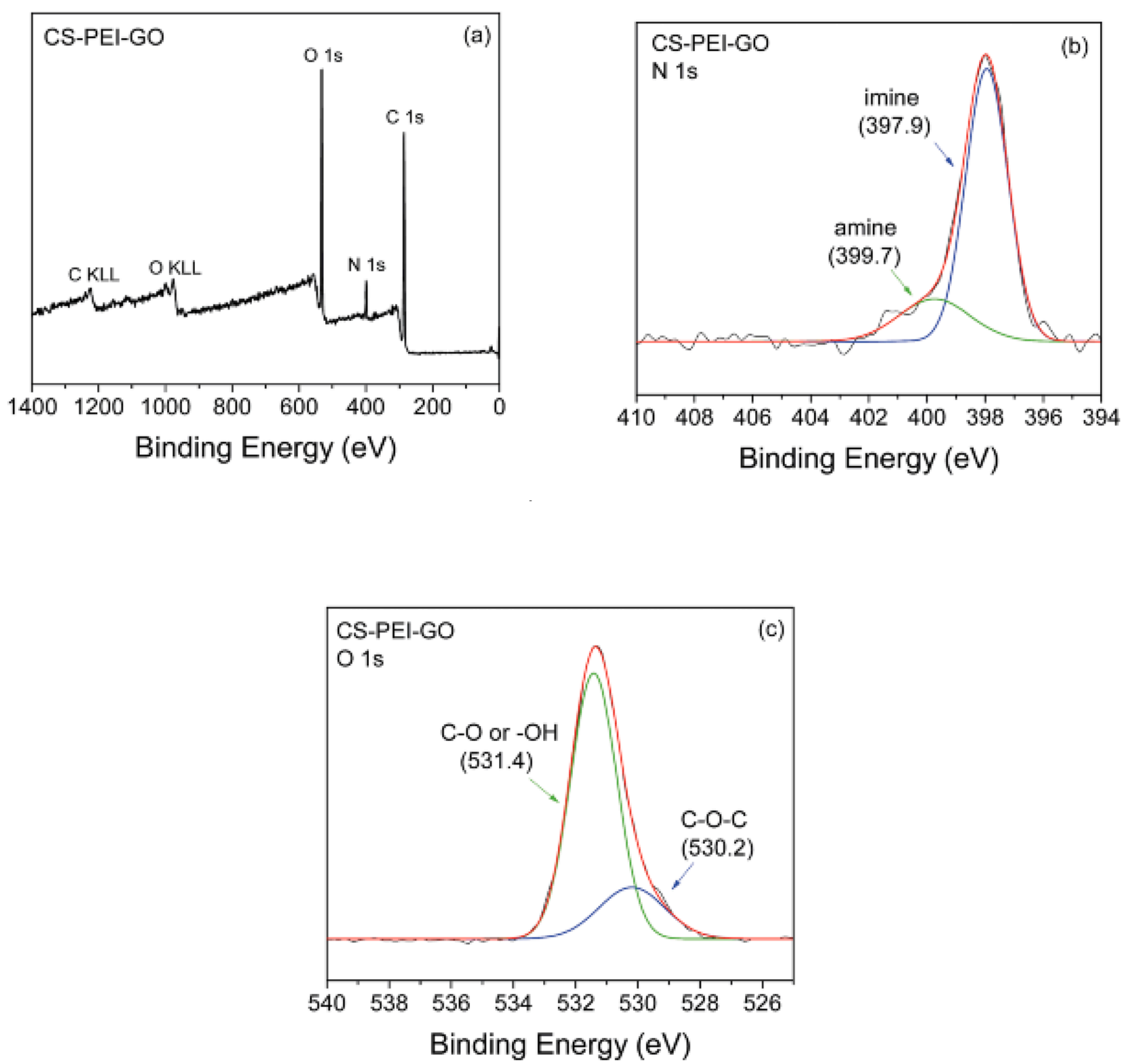

Fig. 11. XPS Spectra of CS-PEI-GO (a). wide scan, (b) N 1 s, and (c) O 1 s (Perez, 2017).

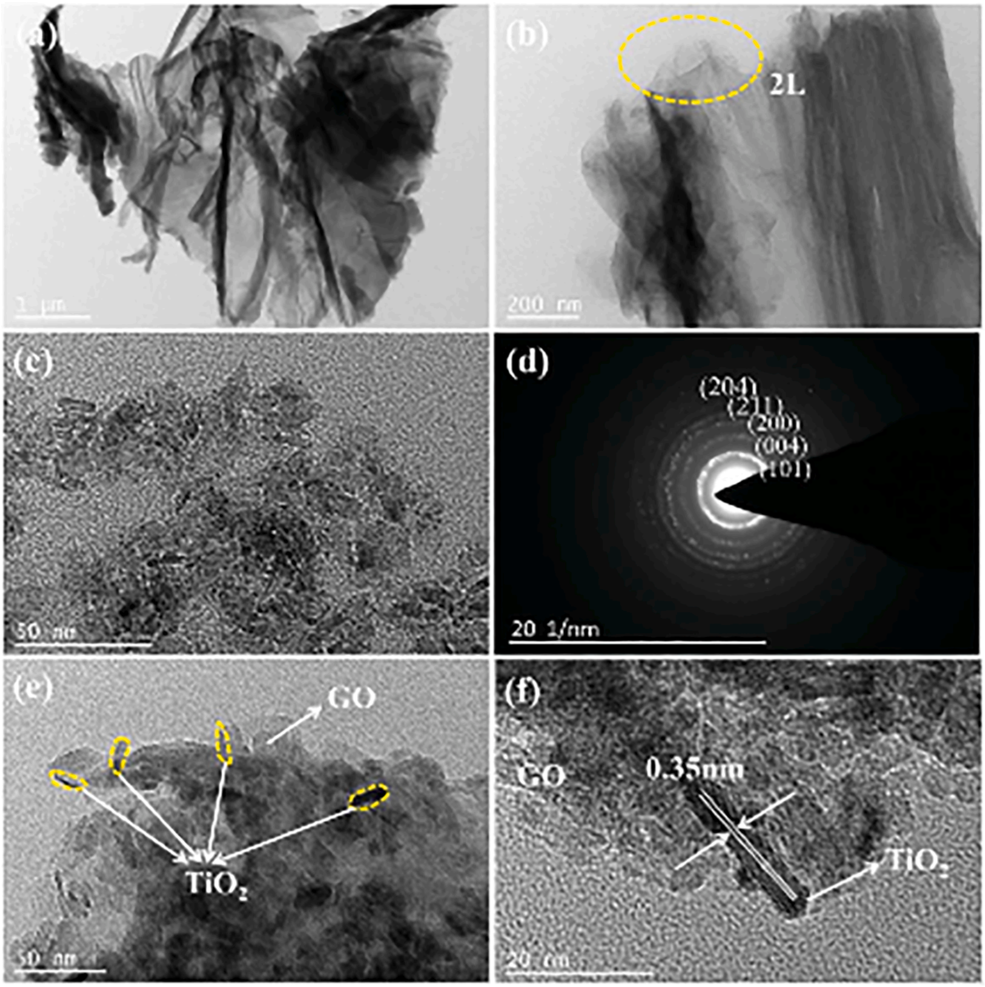

Fig. 12. TEM image of graphene oxide (a & b), TiO_2 with the SAED pattern (c & d) and TiO_2/graphene oxide nanocomposite (e & f) (Zhang, 2018).

nanocomposites decreases, the porosity increases; thus, its magnetization becomes super-paramagnetic. (Lingamdinne, 2016). Dues to supermagnetic property of graphene oxide based nanocomposites, it has helped in the recyclibility behaviour of graphene oxide based nanocomposites to be reused for wastewater treatment thereby reducing the cost associated with treatment of wastewater.

5.3. FT-IR analysis of graphene oxide based nanocomposites

FT-IR spectrum represents the functional groups present in the graphene oxide based nanocomposites. Concerning the principle of FTIR, when a sample is being irradiated with infrared light, there always a reflected or transmitted light which is measured for structural analysis and quantification. This measured light is dependent on wavelength which is absorbed due to vibration and rotation of molecules. For instance, The wave number from 1100 to 1300 cm^{-1} represent the presence of stretching vibration of C-O while the sharp peak ranges from 1400 to 1600 cm^{-1} correspond to epoxy group of graphene oxide in the graphene oxide based nanocomposites. The epoxy group was assigned to the rearranged structure such as D – band sp^3 carbon atoms of disorders and defects and structure of graphite like G - band sp^2 carbons atoms in graphitic sheets of graphene oxide. The wave number from 1650 to 1750 cm^{-1} represents carbonyl (C = O) stretching vibration while the broad peaks from 3000 to 3400 cm^{-1} was assigned to carboxylic acid group of graphene oxide based nanocomposites (Lingamdinne et al., 2019). The wave number from 600 to 500 cm^{-1} indicates spinal magnetic nanocomposites in octahedral/ tetrahedral O-M bonds (Lingamdinne et al., 2019). These primarily indicate the present of magnetic material such as ferrites among others in the graphene oxide based nanocomposites (Lingamdinne et al., 2019). Zhang *et al.,* (Zhang, 2018), reported the FTIR absorption bands for GO, GO/TiO_2 and rGO/TiO_2 nanocomposites in the range of 3750 to 400 cm^{-1}. The GO spectrum showed the presence of different number of functional groups containing oxygen. There is also strong wave numbers at 1070 and 576 cm^{-1} which represent stretching vibration of C-O-C while the band around 1384 cm^{-1} represents bending vibration of C-OH. Also, the band of absorption around 1630 cm^{-1} represent stretching vibration of C = C. When compare the three spectra, it was revealed that there is little presence of functional groups containing of oxygen on TiO_2/GO and TiO_2/rGO surfaces. There was adsorption band at 460.22 cm^{-1} which indicate Ti-O-C bond stretching while band at 523 cm^{-1} was assigned Ti-O vibration. The peak intensity of TiO_2/GO nanocomposites was higher than that of TiO_2/rGO nanocomposites. This was further illustration through Fig. 10.

5.4. XPS analysis of graphene oxide based nanocomposites

The qualitative and quantitative chemical composition of graphene oxide nanocomposites are usually confirmed using XPS. XPS works when a sample is bombarded with an X-ray, some electrons in the sample become excited enough to escape the atom. These excited atoms determined the sample chemical composition (oxidation states and functional groups) of the samples. Liu *et al.,* (Liu, 2017), reported XPS result of modified graphene oxide by goethite (GOF) and established

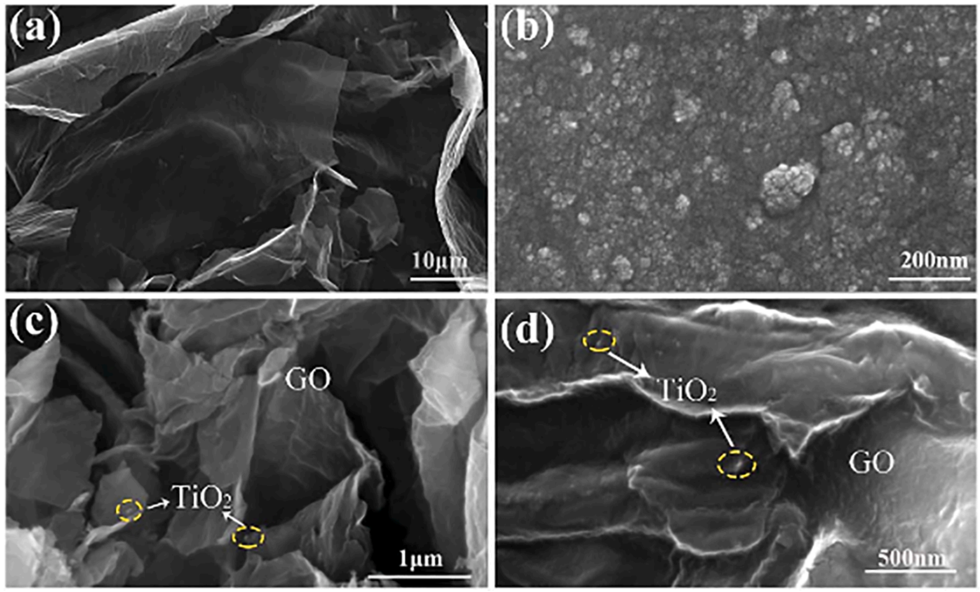

Fig. 13. SEM image of graphene oxide (a) TiO_2 (b) and TiO_2/graphene oxide nanocomposite (c & d) (Zhang, 2018).

that graphene oxide had two main peaks at binding energies of 533 eV and 286 eV which correspond to the bands of O (1 s) and C (1 s) respectively. It was found that the modified GOF (S-type of GOF and C-type of GOF) also had the same peaks in addition to a third peak of Fe 2p at binding energy 726 eV. The peak at binding energy of 531 eV in the O1s spectrum corresponds to the oxygen double bond which confirmed the existence of carboxyl and carbonyl groups. The peak around 532.4 eV was attributed to the single bond of oxygen, which confirmed the existence of epoxy and hydroxyl (Liu, 2017). The spectra of XPS of GO and C-type of GOF revealed three peaks at 286.7 eV, 284 eV, and 287.8 eV, which were attributed to C–O bond, C = C bond, and C = O bond, respectively (Liu, 2017). Comparing with S type of GOF and C-type of GOF, the C-type of GOF has no peak at 287.8 eV, and also the C-type of GOF has no C = O bond, and this result is consistent with the FTIR spectra of C-type of GOF. The binding energy values of 711 and 724.5 eV found from the spectrum of XPS for S-type of GOF and C-type of GOF material for the two iron 2p 1/2 and iron 2p 3/2 are typical of goethite phase Fe(III) (Liu, 2017). Perez *et al.,* (Perez, 2017), also investigated the XPS of CS-PEI-GO nanocomposites and it was shown in Fig. 11a has C 1 s (62.9%), O 1 s (30.5%), and N 1 s (6.6%) peaks at the following binding energies of 284.4 eV, 531.6 eV and 398.0 eV respectively. N (1 s) in Fig. 11b indicates two peaks at binding energies of 399.7 and 397.9 eV which is assigned to amine (–NH_2) and imine (=N-) groups respectively while O (1 s) spectrum also indicates two strong peaks at binding energies of 531.4 and 530.2 eV attributed to C-O or –OH and C-O-C groups respectively. Researchers have reported that peaks at binding energies in the range of 730 – 700 eV confirmed the presence of iron in the magnetic material. Lingamdinne *et al.,* (Lingamdinne, 2017), reported that peaks at the binding energy of 724 eV, 711 eV, 861 eV, and 855 eV correspond to Fe – $2p^1/2$, Fe – $2p^3/2$, Ni – $2p^1/2$ Ni – $2p^3/2$ respectively. While C (1 s) and O (1 s) peaks suggested the presence of carbon and oxygen on the lattice layer of magnetic Nickel ferrite –Graphene oxide composites.

5.5. High Resolution Transmission electron Microscope and high Resolution of Scanning electron Microscope analysis of graphene oxide nanstructured materials.

The size and morphology of nanocomposites are measured via microscopic techniques such as; High Resolution of Scanning Electron Microscope (HRSEM) and High Resolution Transmission Electron Microscope (HRTEM) (Nwosu, 2018). HRTEM is the combination of dark field, bright field, and derivatives of selected area diffraction techniques of analytical TEM. Crucial edge of electron diffraction of TEM over X-ray diffraction is that electron optics can be used to make intensity variation of emerging electrons from sample, which is known as diffraction contrast. This is useful for micro-structural characterization though the preciseness of electron diffraction is comparatively less than X-ray diffraction. Zhang *et al.,* (Zhang, 2020) reported TEM micrograph of modified GO and found that the GO is in form of gauze like sheet structure with corrugated edges and the uniform distribution of Fe_3O_4 nanoparticle was observed on the surface of GO while the Fe_3O_4 particle size ranges between 15 and 35 nm. The author further explained that the Ce-TiO_2 deposited on the surface of GO had average diameter of 10 nm. Mohanta *et al.,* (Mohanta et al., 2020) reported formation of spherical shaped ternary Co_3O_4/TiO_2/GO composites of crystallite sizes around 30 – 50 nm based on HRTEM analysis. Thangavel *et al.,* (Thangavel, 2016), reported HRTEM analysis of ZnS-rGO composites and found a clear ZnS nanospheres uniformly assembled on the surface of RGO. It was found that the ZnS nanospheres distribution was uniformed on reduced graphene oxide sheets maximized the reactive sites and minimize the aggregation of ZnS nanospheres which enhanced the photocatalytic performance reaction. (Zhang, 2018) also reported the presence of multi-layer structures in the HRTEM image of TiO_2/GO composites in Fig. 12. From Fig. 12a and 12b, there was a clear observation of graphene oxide on the special layered surface. While in Fig. 12c, there is similar morphology and size between TiO_2 and GO and in Fig. 12d, it was noticed that TiO_2 has a poly-crystalline structure. The edge of GO sheets was occupied with most of TiO_2 nanoparticles as shown in Fig. 12e-f. These revealed 0.35 nm as the lattice fringe, which corresponds to the anatase TiO_2 lattice spacing of the (1 0 1) plane. It is obvious that graphene oxide barely affects the crystalline and morphology pattern of TiO_2.

Shan *et al.,* (Shan, 2017) reported SEM micrograph of GO and modified GO and found that GO consists of randomly thin, aggregated and crumpled sheet while modified graphene oxide (S-type of GOF and C-type of GOF) clearly indicate surface alterations in the form of porous, rough, and irregular surface. However, compared with S-type of GOF, the surface of C-type of GOF was smooth and layered structure than the S-type of GOF surface. (Zhang, 2018) also investigated the HRSEM images of TiO_2/graphene oxide nanocomposites shown in Fig. 13. In Fig. 13a, it was observed that the shape of GO is irregular with a thin layered structure. While in Fig. 13c and 13c, it was revealed that the

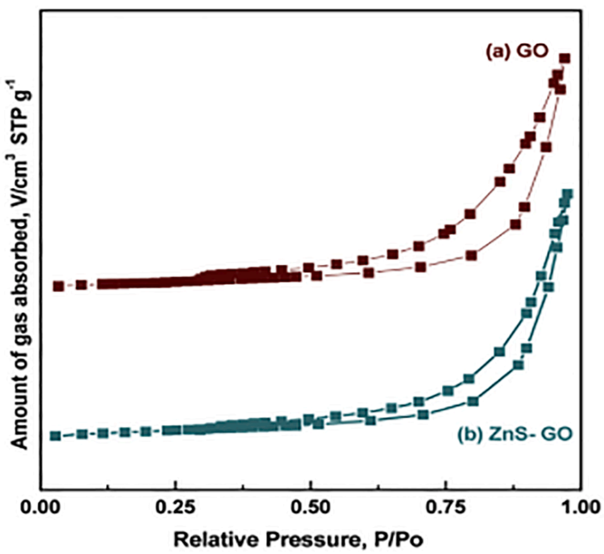

Fig. 14. N_2 adsorption/desorption of N_2 gas (a). Graphene oxide. (b). ZnS-rGraphene oxide nanocomposites (Kashinath et al., 2017).

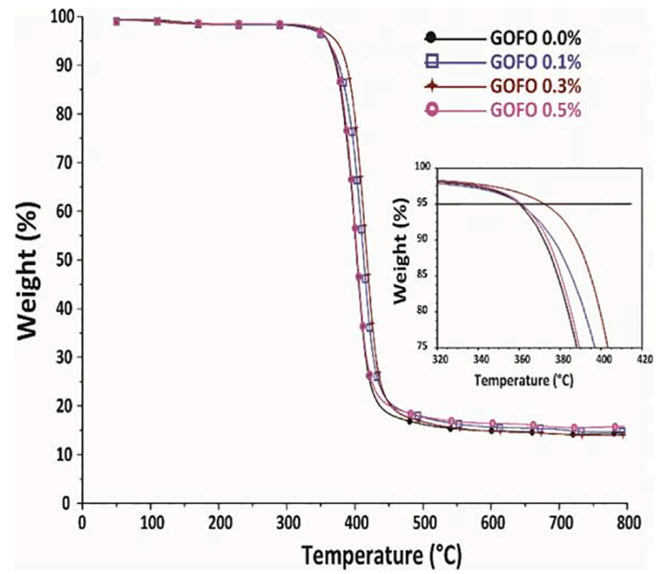

Fig. 15. TGA curves of graphene oxide based nanocomposites under N_2.

layer of GO curled and the well dispersed TiO_2 were anchored on the graphene oxide planes.

5.6. BET analysis of graphene oxide based nanocomposites

The porous structure and surface area of GO based nanocomposites can also be examined using BET technique. The specific surface area of the GO based nanocomposites which include irregular structure and pore wall of a particle is determined at an atomic level via adsorption of an unreactive gas. Most solid and gases (that is the catalyst) interaction is always weak where the solid material are cooled using a cryogenic liquid. The temperatures of the graphene oxide based nanocomposites are constantly kept or through the condition of isothermal while the concentration or pressure of the adsorbing gas is increased. Zhang *et al.,* (Zhang, 2018), also reported the N_2 adsorption/desorption isotherm and BJH pore size distribution of TiO_2/graphene oxide nanocomposite and it was found to exhibit type IV characteristics of a mesoporous material. While the major pore size distribution ranges between 2 and 7 nm with a peak about 5.24 nm. Its surface area was also reported to be 128.41 m^2g^{-1} which is greater than a pure TiO_2 of 59.51 m^2g^1. Hence, the larger the surface area, the more the photogenerated electrons and holes and the greater the photocatalytic degradation efficiency. Kashinath *et al.,* (Kashinath et al., 2017), observed type IV adsorption isotherm for graphene oxide and graphene oxide doped with ZnS possess micro-porous nature. The BET result of ZnS-RGO composite confirmed the formation of mesoporous materials. The distribution curve of pore-size from the isotherm reveals pores value less than 3 nm in the samples. These pores presumably arise from the spaces among the nanoparticles. The specific surface area of 20.92 m^2/g was obtained for ZnS-rGO composites which was higher than 2.24 m^2/g of the pure ZnS nanospheres. It was observed that the data can be attributed to the incorporation of reduced graphene oxide with large area of surface which increased adsorption of reactants through the provision more surface active sites. It was further explained through Fig. 14.

5.7. Thermogravimetric analysis of graphene oxide based nanocomposites

Thermogravimetry (TGA) is a widely used method for determining the thermal stability, composition of organic, inorganic, and synthetic materials (Gerassimidou, 2020). Thermogavimetric analysis refers to the measuring of weight loss during a temperature or heating process that is set by the user. The TGA Thermostep is a thermogravimetric analyzer that determines different parameters such as moisture, volatiles, and ash in a single examination at user-defined temperatures and atmospheres (see Fig. 15) (Alacoque, 2018). This can simultaneously analyze up to 19 samples with a sample weight of up to 5 g at temperatures up to 1000 °C. The handling of crucible coverings is a unique feature of the TGA Thermostep. During analysis, the thermogravimetric analyzer can install and remove the crucible lids (Nikitin, 2021). This property, for example, enables for the precise assessment of coal's volatile content. Several researchers have analysed graphene oxide based nanocomposites using thermogravimetric analysis. Fan (Fan, 2019) reported that the addition of the proper content of graphene oxide modified with fluorinated-diol (GOFO) enhanced the performance of epoxy resin. It was further explained that the epoxy composite tensile and flexural modulus increased by 12.52 % and 62. 85 % respectively with 0.5 wt% GOFO loading. Epoxy composite with 0.3 wt% GOFO shows high thermal stability. The $T_{5\%}$, $T_{50\%}$, and T_{dec} were 13 °C, 15 °C, and 13 °C, respectively, higher than pure epoxy.

5.8. Raman spectroscopy analysis of graphene oxide based nanocomposites

Raman spectroscopy is a tool for studying molecular bonding in materials that is extremely sensitive to structural changes (Shao and Zenobi, 2019). Another scattering approach is used, except the photons from a laser source, typically in the infrared to UV wavelengths (Kumar, 2020). A small percentage of the incident photons undergo Raman scattering, loses energy when the sample's vibrational modes are excited (Kumar, 2020). A spectrum is created by detecting scattered photons. In comparison to the other techniques discussed here, Raman spectroscopy often offers a significantly greater depth of investigation. However, the additional information received is particularly important for comprehending both polymers and nanomaterials, such as graphene oxide and carbon nanotubes, where the depth scales correlate well. Several researchers have employed the application of Raman spectroscopy analysis of graphene oxide based nanocomposites. Sharma *et al.,* (Sharma, 2019), discussed Raman spectroscopy analysis of graphene oxide and L-Glutathione-reduced graphene oxide to give information about the structural disorders, crystallization, defects and quality of carbon materials during oxidation and then reduction of the samples. It was also reported that the D band of GO is at 1344 cm^{-1} which associated with the disorder due to oxygen moieties and G band at 1595 cm^{-1} due to C – C stretching while a peak of 2697 cm^{-1} in L-glutathione-reduced

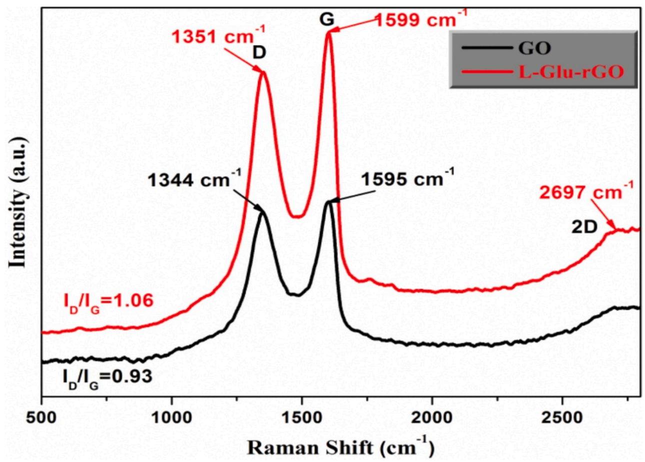

Fig. 16. Raman Spectra of GO and L-Glu-rGO.

graphene oxide affirmed the presence of graphene oxide structure by corresponding to 2D band as shown in Fig. 16.

6. Application of graphene oxide based nanocomposites in advanced oxidation process.

The use of advanced oxidation processes (AOPs) have been widely employed for the treatment of water and wastewater based on the utilization of free reactive species like hydroxyl radicals, ozone, superoxide to degrade organic pollutants in the water system to less toxic minerals (Miklos, 2018). The radical commonly employed in advanced oxidation is hydroxyl which is one of the most powerful agents with oxidizing potential $(E^{\circ})_{(\cdot OH/H2O)}$ of 2.8 V after fluorine (Ighalo, 2021). Hydroxyls radical always attack the organic compound at the time of generation which causes the degradation of compounds through hydroxylation, dehydrogenation and redox reaction (Miklos, 2018). The following are the examples of advanced organic processes used for degradation of one or more organic compounds in aqueous medium; Fenton (Zhang, 2019), electro-Fenton (Akyol, 2019), photo- Fenton (Garcia-Muñoz, 2020), sono-Fenton (Xu, 2020), photoelectro-Fenton (Alcaide, 2020), ozonation (Tanatti, 2019), photocatalysis (Dutta, 2017) among others used for mineralization of various pollutants. This session will focus on photocatalysis and photo-Fenton.

In recent time, due to the similarity of AOPs of sulfate radical and hydroxyl radical, sulfate radical has received much attention (Soltani and Lee, 2017). Sulfate radical has oxidation potential of 2.1 V which is of similar with that of hydroxyl radicals; common precursors are persulfate and peroxymonosulfate ions in aqueous medium which is soluble and stable in aqueous medium. These precursors generated sulfate when ultrasound, heat, UV light are present as activated agents (Nidheesh and Rajan, 2016). Recently, articles were published on graphene-oxide based materials application in AOPs for the treatment of water and wastewater (Zubir, 2015). Graphene oxide-supported AOPs application for the mineralization of organic pollutants is based on the fact that graphene oxide has a large surface area, higher mobility as charge carrier and chemical stability among others which improved the efficiency of the AOPs (Deng and Zhao, 2015). Therefore, graphene oxide based nanocomposites has become a highly interested research area in AOPs for the treatment of water and wastewater. Fig. 17 shows various advanced oxidation process supported by GO based materials.

6.1. Photocatalysis

Fujishima and Honda had earlier published an article on splitting of water (Fujishima and Honda, 1972) and since then researchers have explored different semiconductor photocatalysts for wastewater treatment. For instance, TiO_2 particularly (rutile and anatase phase) was utilized for cyanide ion photocatalysis (Frank and Bard, 1977). TiO_2 has been widely used as photocatalyts due to its peculiar properties such as excellent photoactivity, good chemical and biological stability, non-toxic, low cost, super-hydrophilicity amongst others (Norhayati, 2016). Other metal oxides such as Fe_2O_3, WO_3, ZnO among others and their combination have been widely applied in the field of photocatalysis for the treatment of water and wastewater (Solis-Casados, 2018). However, there have been several challenges associated with metal oxide photocatalyst such as TiO_2 with wide band gap of>3 eV which will require high energetic UV irradiation for activation (Zhang, 2017). Other shortcomings include high agglomeration tendency, poor stability of the active charge carriers due to high rate of recombination,

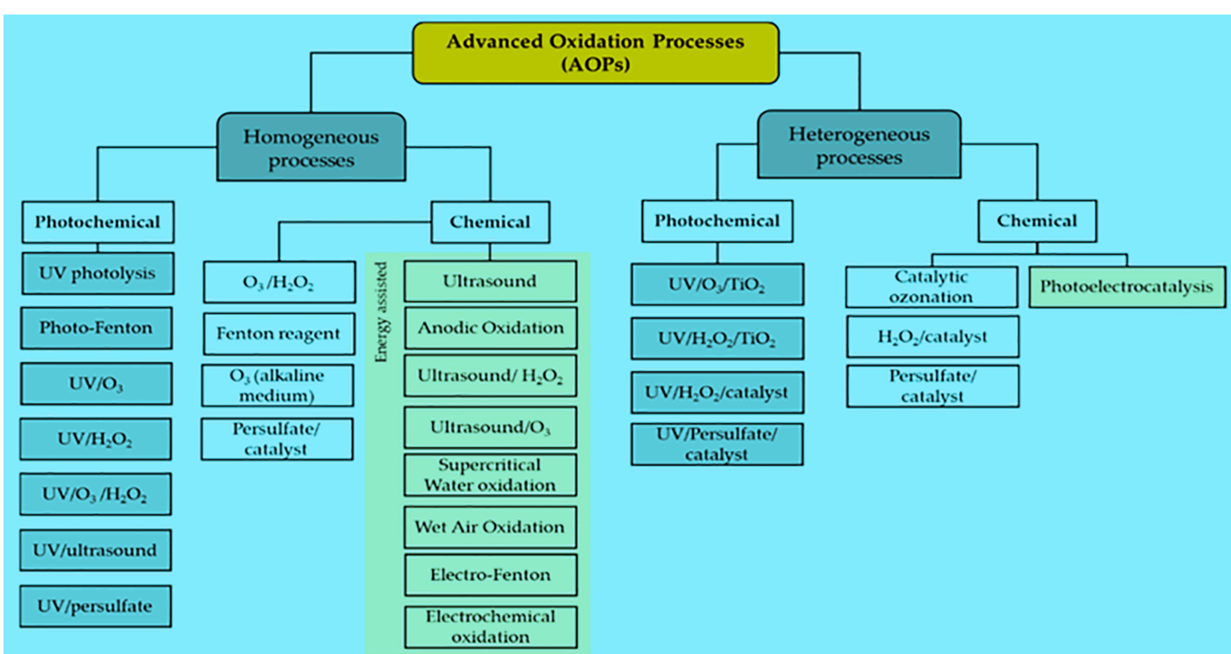

Fig. 17. Different types of advanced oxidation process (Gopal, 2020).

Table 2
A brief summary of research studies on photocatalytic degradation using graphene oxide based nanocomposites.

Nanocomposites	Reaction conditions/Pollutants	Research findings	Research gaps	References
magnetic-GO/Ce/TiO_2 (MCT)	Tetracycline (TC), 300 W Xe lamp, 25 mg/L of initial concentration, 60 min, precursor: 50 mL of Tetrabutyl titanate, Ce(NO3)3 and 16 mL of isopropanol.	− 82.9% removal of TC -facile method was used to prepare MCT hybridized composite. -It exhibited good adsorption capacity, magnetic separability and high visible-light photoactive photocatalyst in breaking down of TC.	-Different light source was not investigated on the photocatalytic activities and the synthesis was not through green synthesis	(Cao, 2016)
Graphene/TiO_2/ZSM-5	Oxytetracycline (OTC). 300 W visible lamps (light intensity: 1385 W/m^2), 30 min, precursors: Titanium dioxide, graphene and Zeolite.	−100% complete degradation was achieved at 180 min -The bio-toxicity of the degraded intermediates of OTC.	-The recycleability of the nanocomposite was not studied synthesis	(Hu, 2016)
Graphene sand composite and chitosan supported BiOCl	Ampicillin (AP) and Oxytetracycline (OTC) 260 and 350 nm respectively, 25–35 °C. precursors: 1.0 g of sugar cubes, 0.5 g of sand, 1 g of $BiCl_3$.	− 90.0% degradation was removed at 120 min. -simultaneous adsorption and photocatalysis has synergistic effect on process. -Complete photo-mineralization of antibiotics was attainted under solar light	- Biotoxicity was not analysis.	(Priya, 2016)
Bi_2O_3/BiOCl supported on graphene sand composite and chitosan	Oxytetracycline (OTC) and Ampicillin (AP) 260 and 350 nm respectively, 25–35 °C. precursors: 1 g of $BiCl_3$, 50 mL of KBH_4 (5.0×10^{-3} mol/dm^3), 1.0 g of sugar cubes, 0.5 g of sand.	−95.0% of AP was removed in 60 min -Antibiotics were completely mineralized under solar light	-Different light sources were not investigated on the photocatalytic activities.	(Priya, 2016)
Surface modification of graphene oxide by goethite (GOF)	Tylosin (TYL) xenon long-arc lamp is 300–800 nm, 3 h, 0.45 μm membrane filter, detection limit 10 μg/L. precursors: 5 M KOH, 0.5 M of $Fe(NO_3)_3$.	-Graphene oxide and goethite complex were synthesized by hydrothermal and in situ synthesis method -The degradation efficiency of TYL achieved at 84 % for 120 mins.	- Biotoxicity was not analysis. -recycle of the nanocomposite was not checked	(Shan, 2017)
Cobalt promoted TiO_2/GO (CTG)	Oxytetracycline (OTC) and Congo Red (CR) 300 W Xe solar simulator, 6000 rpm, 15 min, 100 mW/cm^2. Precursors: 0.4 mol cobalt Nitrate, 50 mL deionized H2O, 50 mL solution of 0.013 mol titanium isopropoxide.	−91.0 % of the pollutants were removed at 90 min. -Titania derived nanocomposite prepared through hydrothermal and sol–gel routes revealed excellent performance for the photocatalytic degradation of two important exemplar water pollutants; OTC and CR	-Synthesis procedure was not through green synthesis -recycle of the nanocomposite was not checked	(Jo, 2017)
3D ZnS-RGO	Norfloxacin (NOR), 300 W Hg vapor lamp, 4000 rpm for 5 min, wavelength of 272 nm, 0.22 μm membrane filter. Precursors: 2 g of graphite, 0.26 g $ZnCl_2$ and 0.3 g thiourea,	−92.0% of the pollutant was removed in 4 h -The ZnS-rGO composites are synthesis via facile hydrothermal. -The ZnS-rGO composites revealed excellent photocatalytic performance for degradation of NOR degradation.	- Biotoxicity was not analysis. -recycle of the nanocomposite was not checked	(Bai, 2017)
ZnO-GO/NC	Ciprofloxacin hydrochloride (CF), 100 Mw/cm^2, 90 min, 266 nm, precursors: 0.01 M zinc acetate dehydrate, graphite powder, cellulose.	−98.0% of the pollutant was degraded -The reusability of ZnO-GO/NC after five consecutive cycles indicated it to be a potential candidate for the degradation and removal of CF.	- Biotoxicity was not analysis. -recycle of the nanocomposite was not checked.	(Anirudhan and Deepa, 2017)
MOF/GO	Amoxicillin 300 W Xe lamp, 420 nm cut-off filter, 25 °C, pH 3, flow rate of 1 mL/min. precursors: 1.92 mmol of $In(NO_3)_3 \cdot xH_2O$ and 0.645 mmol of BDC-NH_2.	-The MIL-68(In)–NH_2/GrO composite photocatalyst was prepared via a sample solvothermal method −80 % TOC removal and 93 % degradation	-The author did not investigate band energy and effect of different light sources.	(Yang, 2017)
Graphene-based TiO_2 composite	Antibiotic-resistant bacteria, Antibiotics, pilot unit 10 m^3d^{-1}, 100 m^2, 0.4 μm, 9 h, range of pH 5.2–6.2, 500 rpm. Precursors: Clarithromycin, erythromycin, sulfamethoxazole, tetrabutyl titanate and graphite powder.	-Complete bacterial inactivation was observed after 120 min of treatment. -There was no E. coli re-growth observed after 180 min.	- Real effluent was not use in degradation analysis and green synthesis was not use in synthesis of TiO_2	(Karaolia, 2018)
N-doped TiO_2/reduced graphene oxide	Tetracycline hydrochloride (TC), 300 W Xe-arc lamp with a 400 nm cutoff filter, 30 min. precursors: 5 ml acetic acid, 12 mL tetrabutyl titanate and graphite powder.	−98.0% removal of TC in 60 min. -photo-reduction method to prepared N-TiO_2/rGO -N-TiO2/rGO composite exhanced visible-light photocatalytic activity	-Different light sources were not investigated on the photocatalytic activities.	(Tang et al., 2018)
RGO-ZnTe	Tetracycline (TC), AM 1.5, 100 mW/cm^2, 1 h, precursors: graphite powder, zinc acetate dehydrate and Sodium tellurite.	-RGO-ZnTe was synthesis by a single pot one step solvothermal process −65.0% removal of TC.	-The author did not investigate band energy and different light sources	(Chakraborty et al., 2018)

(continued on next page)

Table 2 (*continued*)

Nanocomposites	Reaction conditions/Pollutants	Research findings	Research gaps	References
$BiVO_4$ /N-rGO	Metronidazole (MD), 500 W of tungsten lamp, 30 min, λ > 420 nm. Precursors: 50 mg GO, $Bi(NO_3)_3{\cdot}5H_2O$ and NH_4VO_3.	-Nitrogen doped rGO/$BiVO_4$ composite catalyst was synthesized in a single step. −95.0% of MD was degraded within 240 min.	- Biotoxicity was not analysis. -recycle of the nanocomposite was not checked	(Appavu, 2018)
BiOCl-$Bi_{24}O_{31}Cl_{10}$/rGO	Fluoroquinolone (FQ), 400 W halogen lamp, wavelength 315 nm, 120 min. precursors: flake graphite powder and bismuth nitrate pentahydrate	-Sono-solvothermal method was used prepared the nanocomposites. −90.0% removal of FQ	-Different light sources were not investigated on the photocatalytic activities.	(Shabani, 2019)
TiO_2/nitrogen doped holey graphene	Cefixime (CF), wavelength range 200 to 800 nm, 3500 rpm, 30 min, λ_{max} 287.5 nm, precursor: 2g flake graphite and 1g $NaNO_3$, 2g of urea.	- The photocatalytic degradation was studied under sun light radiation. −92.3% of CF was degraded for 90 min	-proper optimization study to investigate the effect of stirring speed and different calcined temperature were not investigated	(Shaniba, 2020)
ZnO-CdO-RGO	Bisphenol A (BPA), Thymol blue (ThB) and Ciprofloxacin (CFn). UV light irradiation,	98.5 %, 98.38 % and 99.28 % of BPA, ThB and CFn were degraded for 180 min, 120 min and 75 min respectively. The synthesis approach is simple refluxing method	The band energy and different light sources were not examined	(Kumar et al., 2022)
ZnO-CdS-RGO	Hexavalent chromium (Cr (VI)). The nanocomposite was optimized. Room temperature.	93.2 % of Cr(VI) was degraded after five cycles of uses.	The synthesis approach is not green synthesis and different calcined temperature were not investigated	(Zhao, 2022)
ZnO-rGO	Methylene blue (MB). The GO was synthesis by hammer and offeman process using 1:1.	99 % degradation of MB in 60 min. 36.1 kJ/mol and 13.1 kJ/mol were calculated as the apparent and true activation energy respectively.	- Biotoxicity was not analysis. -recycle of the nanocomposite was not checked.	(Nisar, 2022)

difficulty of recovery process after utilization for wastewater treatment (Pan, 2020). In order to enhance the semiconductor efficiency, several approaches have been adopted such as doping with non-metal or metal ions, amalgamation of metal oxide with electron scavenging agents, coupling, composite formation and even modification of the surface by chemical or physical routes (Ighalo, 2021). These modification strategies will greatly reduce the band gap and extend the photocatalytic response in the visible region of the solar spectrum (Bhanvase et al., 2017). Among these several routes, formation of composite using carbonaceous material have been majorly drawn attention in the recent time due to its semi metallic properties and ability to lower band gap of metal oxide (Ashouri, 2019).

Additionally, Graphene oxide which belongs to carbonaceous material has been used a dopant due to its hydrophilic groups such as carboxylic, epoxide, and hydroxyl groups on its surface through graphene (Ray, 2015). Graphene oxide can absorb pollutants and form stable complexes, causing difficulties for the separation and recovery of due its hydrophilic nature (Kumar and Jiang, 2017). To control these separation difficulties, magnetic functionalization of GO has been proposed as an alternative solution (Pu, 2018). Some studies have been done on development of magnetic GO composites for effective applications, such as treatment of water, drug delivery, and energy storage (Chowdhury and Balasubramanian, 2014). Therefore, Graphene oxide based nanocomposites is expected to have a high surface area and reduced agglomeration of metal oxide due to their weak van der Waals forces (Khan, 2015). Researchers have considered coupling of two or more metal oxides as a viable approach for the enhancement of catalytic activity during degradation of organic pollutants. For instance, Tayel *et al.,* (Tayel et al., 2018), found that loading graphene oxide over titanium dioxide, enhanced the titanium dioxide catalytic activity by 1.2 factor (Tayel et al., 2018). The enhancement of titanium dioxide photocatalytic activity was primarily due to the Graphene oxide electron accepting and transporting properties (Zheng, 2013). The electrons accepted by Graphene oxide was generated on the titanium dioxide surface in the presence of light and causes electron-hole recombination reduction which enhanced more active holes production (Ajala, 2022). The second reason behind the TiO_2 photocatalytic activity enhancement was linked to the band gap width reduction of TiO_2 upon graphene oxide addition. This band gap reduction enables the photocatalyst to produce the radicals even at longer wavelengths. For this enhancement, the graphene oxide concentration is also an important parameter. At lower GO concentrations, TiO_2 were uniformly distributed over graphene oxide surface and enhanced the photocatalytic activity. On the contrary, at higher GO concentrations, aggregation of photocatalyst occurs, which reduced the catalyst efficiency due to increase in mass transfer restrictions. Cao *et al.,* (Cao, 2016) reported photocatalytic degradation of tetracycline using magnetic-GO/Ce/TiO_2 and found that 82.9 % of tetracycline was degraded. Also, Priya *et al.,* (Priya, 2016) reported photocatalytic degradation of ampicillin and oxytetracycline by Bi_2O_3/BiOCl supported on chitosan and graphene sand composite and it was revealed that 95 % removal of ampicillin was achieved in 60 min through solar light. Other previous studies on the photocatalytic behaviour of GO based nanocomposites are summarized in Table 2.

From table 2, different graphene oxide based nanomaterials has been synthesised via doping, coupling among other for formation of photocatalyst. These photocatalyst has been reported to be highly efficient with minimum of 90 % degradation of any kind of organic compound pollutants. However, several parameters such as band gap energy, biotoxicity analysis and recycle of the nanomaterials among others were not studied. Toxicity test of the treated water should be given utmost priority.

6.2. *Photo-Fenton process*

This is an AOPs which involves the combination of hydrogen peroxide and iron ions with ultraviolet radiation to generate hydroxyl radicals and further increase the rate of degradation of organic pollutants (Wu, 2021). It has been established that the presence of light improved the performance of the Fenton oxidation based on the increase concentration of hydroxyl radicals produced by hydrogen peroxide decomposition (Xavier, 2016). Graphene related based materials such as Graphene, GO, rGO categorized as heterogeneous catalyst have applied in photo-Fenton system to improve the overall performance of the catalyst (Xie, 2020). The following graphene related based materials have been employed in photo-Fenton process; α-FeOOH/rGO (Lin, 2019), $ZnFe_2O_4$/rGO (Gopi, 2020), amorphous $FePO_4$/graphene oxide (Lu, 2016) and α-Fe_2O_3/GO (Liu, 2017) among others to improve the performance in the catalysis mechanism. Apart of the performance in

Table 3
A brief summary of research studies on photo-fenton degradation using graphene oxide based nanocomposites.

Nanocomposites	Pollutants/ reaction conditions	Research findings	Research gaps	References
Fe_3O_4-GO	Phenol/pH 5.0, 14,000 rpm, 500 W xenon lamp, 100 mW/cm^2, 30 min. Precursors: 1.0 g of powdered graphite flakes, 0.5 g of sodium nitrate, 2.0 mmol of $FeCl_2 \cdot 4H_2O$ and 4.0 mmol of $FeCl_3 \cdot 6H_2O$.	-It was observed that Fe_3O_4-GO showed high catalytic activity after five cycles -the enhanced catalytic activity is attributed to the synergetic effect of GO and Fe_3O_4	-The author did not investigate the hybrid AOPs of photocatalytic activities.	(Yu, 2016)
Zn-doped Fe_3O_4	Rhodamine B (RhB) and Cephalexin/350 W of Xe lamp with a $\lambda > 420$ nm cutoff filter, 5000 rpm, 5 min, precursor: 1.08 g of $FeCl_3 \cdot 6H_2O$ and 0.272 g of $ZnCl_2$ and 2.312 g of amoniacetate.	-It involves irradiation of visible light. -Easy separation and reuseability through external magnetic field −97% of RhB and about 90% of cephalexin were degraded for 60 mins and 180 mins. And only18% removal of cephalexin and 26 % removal of RhB through the pure Fe_3O_4	-Different light sources were not investigated on the photocatalytic activities.	(Nguyen et al., 2017)
α-Fe_2O_3/GO	Methylene Blue(MB)/ 100 W high-pressure mercury lamp with a main wavelength of 365 nm, 1.4 mW/cm^2, 20 °C. Precursors 0.1 g GO, 4.04 g of $Fe(NO_3)_3 \cdot 9H_2O$ and 2.4 g of urea	-it was synthesis via facile hydrolysis method -Toxicity of MB was reduced after photocatalytic degradation.	-recycle of the nanocomposite was not checked	(Liu, 2017)
Fe_3O_4-Mn_3O_4/rGO	Sulfamethazine/ 40 mL of SMT solution, 160 rmp, 0.22 μm, flow rate 1 mL/min, 30 °C, 275 nm. Precursors: diethyleneglycol, $Mn(CH_3COO)_2 \cdot 4H_2O$, $FeSO_4 \cdot 7H_2O$ and $Fe_2(SO_4)_3$.	-The removal efficiency of SMT was about 98 % at optimal conditions.	-Biotoxicity was not investigated.	(Wan and Wang, 2017)
Ag/AgCl/Fh	Bis-Phenol (BPA)/ A 5 W LED lamp (148.5 mW/cm^2), pH 3, 0.22 μm membrane filters. Precursors: 30 mL of NaOH (4 mol/L) and 50 mL of Fe $(NO_3)_3 \cdot 9H_2O$ (1 mol/L).	-The degradation rate constant of BPA over 6 % Ag/AgCl/Fh nearly about 5.1 times as high as thst of pure Fh	-Real effluent was not use in degradation analysis	(Zhu, 2018)
CdS/rGO/Fe^{2+}	Phenol / 300 W of xenon lamp irradiation ($\lambda >$ 420 nm) for 1 h. Precursors: 1.0 g of $NaNO_3$, 2.0 g of graphite powder, 0.1583 g of thiourea and 0.1589 g of cadmium acetate.	-The degradation efficiency was high for phenol. -Photo-Fenton reaction was efficiency performed and stably at natural pH	-proper optimization study to investigate the effect of stirring speed and different calcined temperature were not investigated	(Jiang, 2019)
Activated Carbon/ $CoFe_2O_4$	Reactive Dye/ pH range 2–11, 400 rpm, 30-W (UV-C) mercury lamp, 10–100 min, initial dyes concentration 5–100 mg/L, 21 ± 1 °C Precursors: $FeCl_3 \cdot 6H_2O$, $CoCl_2 \cdot 6H_2O$ and activated charcoal.	−100 % and 98 % removal rates were achieved for reactive red 198 and COD respectively	-The study revealed that effect of stirring speed, time and solution pH was not investigated on the particle size formed	(Heidari, 2019)
NGO-Fe_3O_4	Norfloxacin (NOR). The nanocomposite was synthesis using hydrothermal-co-precipitation methods.	−100 % of NOR was degraded within 13 min. The nanocomposite showed stable catalytic activity in recycling.	-Different light sources were not investigated on the photocatalytic activities.	(Wu, 2022)
$FeWO_4$/Bi_2MoO_6	Tetracycline antibiotic (TA) and methylene blue (MB). The catalyst dose of 30 mg/50 mL spiked with 20 μL of H2O2 (30 % v/v).	97% degradation of TA and 99 %degradation of MB within 90 min.	-Biotoxicity was not investigated.	(Kumar and Dutta, 2022)

catalysis mechanism, graphene oxide also improves performance of the Photo-Fenton process by generation of hydroxyl radical. For instance, Gopi *et al.,* (Gopi, 2020) established that hydroxyl radicals were generated by two ways either through Photo-Fenton or Photocatalytic reactions. The authors further explained that on the surface of $ZnFe_2O4$, the light energy generated hole-electron pairs and the graphene oxide received the generated electrons and negative charge. Through this charge, graphene oxide activated the hydrogen peroxide to generate hydroxyl radicals in the photo-Fenton system. The generation of hydroxyl radicals is referred to as photocatalytic method while electron photo-generation reacts with different type of ferrous ions and further with hydrogen peroxide to produce hydroxyl radicals. For instance, Yu *et al.,* (Yu, 2016) investigated the photo-fenton potentials of Fe_3O_4-GO for degradation of phenol and found that the synthesized nanocomposites exhibited high catalytic activity after five cycles. Also, Liu *et al.,* (Liu, 2017) reported hydrothermal synthesis of α-fe_2O_3/GO for the photo-fenton breakdown of methylene blue and revealed 98 % removal of the Methylene blue. Other previous studies on the photo-fenton behaviour of GO based nanocomposites are summarized in Table 3.

From table 3, different Fe ions have been coupled with graphene oxide as photo-fenton agents of higher efficiency in the degradation of several organic pollutants. There are others factors which were not examined in most research especially biotoxicity analysis, different light sources and recyclability potentials of the nanomaterials among others.

7. Application of graphene oxide based nanocomposites in hybrid advanced oxidation process.

Graphene oxide based nanocomposites have been widely studied due to its improvement in hybrid AOPs (Muruganandham, 2014). Hybrid AOPs is a technique which combined two types of advanced oxidation process for degradation of inorganic and organic pollutants in water and wastewater treatment (Kumar et al., 2020). The following are the types of hybrid advanced oxidation process with graphene oxide based nanocomposites; Photoelectrocatalysis (Pan, 2020), Photocatalytic ozonation (Chávez et al., 2020), Sonophotocatalysis (Chakma, 2020) and combination of photocatalysis and photo-Fenton among others. Photoelectrocatalysis is the combination of electrocatalysis and photocatalysis for degradation of various organic and inorganic pollutants (Pan, 2020). Generally, photoelectrocatalysis system consists of photocatalysts as an anode material exposed to light source (UV light or sun light) for effective degradation of pollutants in the aqueous medium. Photoelectrocatalysis is more advantageous than photocatalysis due to easy separation of holes and electrons in the present of an electrical charges (Pan, 2020). Graphene oxide based nanocomposites has been employed in photoelectrocatalysis as working electrode and it was found that degradation efficiency of the combined system greatly improved compared to individual system. For instance, Yuan *et al.,* (Yuan, 2018) synthesized ternary polyaniline-GO/TiO_2 hybrid films and applied as photoanode in the photoelectrocatalytic for water reduction. Compared

Table 4
A brief summary of research studies on hybrid advanced oxidation process using graphene oxide based nanocomposites.

Hybrid Advanced Oxidation Processes	Titania-GO based nanocomposites	Pollutants/Reaction conditions	Research findings	Research gap/ shortcomings	References
Sonocatalysis	MIL-101(Cr)/RGO/$ZnFe_2O_4$	Congo Red(CR), Methylene blue (MB) and Rhodamine B (Rh. B)/ initial concentration of 25 mg/L, 25 °C, 30 min. Precursors: graphene oxide (0.1 g), terephthalic acid (0.498 g) Cr $(NO_3)_3{\cdot}9H_2O$ (1.2 g), $ZnCl_2{\cdot}2H_2O$ (0.28 g), and $FeCl_3{\cdot}6H_2O$ (1.08 g).	99 % degradation of CR and over 98 % of MB and Rh.B.	-Real effluent was not use in degradation analysis	(Nirumand, 2018)
Catalytic ozonation	N-TiO_2/Graphene/Au and N-TiO_2/Graphene/Ag	Diazinon (DZ) pH 4–9, Precursors: 0.25 g N-TiO_2, 0.08 g graphene, Au or Ag, 60 mL 2-propanol, and 0.01 g magnesium nitrate.	the degradation rate of DZ was nearly 100 %	-Toxicity and recycleablility of the nanocomposite was not investigated	(Ayoubi-Feiz et al., 2019)
Photoelectrocatalysis	N-TiO_2/Graphene/Au and N-TiO_2/Graphene/Ag	Diazinon (DZ) pH 4–9, Precursors: 0.25 g N-TiO_2, 0.08 g graphene, Au or Ag, 0.01 g magnesium nitrate and 60 mL 2-propanol.	76.7 % degradation for N-TiO2/G/Au and 81.1 % for N-TiO2/G/Ag.	-proper optimization study to investigate the effect of stirring speed and different calcined temperature were not investigated	(Ayoubi-Feiz et al., 2019)
Sonophotocatalysis	Au/B-TiO_2/rGO	Tetracycline (TC)/ Sonicator capacity 40KHz, 25 L, 300 W halogen lamp precursors: 104.41 mg Boric acid, 133.02 mg Gold(III) chloride, GO.	100 % Degradation of Tetracycline was achieved with 1.3 folds synergistic effect when ultrasound coupled with photocatalysis in 1 h.	-Biotoxicity of the nanocomposite was not investigated and the nanocomposite was not synthesis through green synthesis.	(Vinesh et al., 2019)
Photoelectrocatalysis/ filtration	Poly (3, 4-ethylenedioxythiophene) modified polyvinylidene fluoride membrane	tetracycline hydrochloride (TCH) voltage of 3 V, visible light irradiation precursor: polyvinylidene fluoride, $FeCl_3{\cdot}6H_2O$ Poly (3, 4-ethylenedioxythiophene).	The Results revealed that the photoelectrocatalytic removal of TCH was 1.6 and 7.9 times higher than that of photocatalysis and photolysis respectively. The stability tests and anti-interference in continuous filtration process also revealed that the dissolved organic matters were removed by 30 % in fluctuation on removal rate.	-proper optimization study to investigate the effect of different parameters were not investigated	(Liu et al., 2019)

with pristine titanium oxide electrode, it was observed that the ternary hybrid films of GO, titanium oxide and polyaniline layer exhibited better photoelectrocatalysis activity and generated higher rate of hydrogen compared to most reported titanium oxide based nanophotoctalyst. The mechanism of Photoelectrocatalysis analysis insinuated occurrence of charge transfer efficiency at the polyaniline - graphene oxide – titanium oxide interface due to the potentials band matched. Polyaniline served as both transporter and electron collector and counter electrode readily received the electrons to reduce water into H_2 under certain bias voltage. In addition, the data from other studies suggested that the used of electrolyte played a vital role in photoelectrocatalysis reduction of water (Ajala, 2022).

Catalytic ozonation (combination of ozonation and photocatalytic ozonation) have been proved to overcome several disadvantage of process of ozonation such as energy requirement and high operational cost. Heidarizad and Şengör (Heidarizad and Şengör, 2017. 2017.) reported catalytic ozonation as a potential AOPs for degradation of pollutants from wastewater. The data revealed that the catalytic ozonation significantly enhanced phenol mineralization compared to ozonation in the absence of catalyst. Also, Heidari *et al.,* (Heidari, 2019) found that the modified GO/MgO demonstrated high rate of adsorption of methylene blue.

Sonochemical method is an innovative method involving application of ultrasound for the degradation of organic pollutants in water and wastewater (Govindasamy, 2019). The phenomenon created from the application of ultrasound is referred to as acoustic cavitation which caused the degradation of organic pollutants via bond breakage at high pressure and temperature (Govindasamy, 2019). The generated radicals via ultrasound dissociated the water and other organic pollutants. The used of graphene oxide related materials in sonochemical treatment of water and wastewater is limited to the catalyst modification. GO was employed to serve as a supporting material for heterogeneous and homogeneous catalysts. The support provided by graphene materials improved the efficiency of the processes of sonochemical. Other previous studies on different hybrid advanced oxidation process were summarised in Table 4.

8. Conclusion and future perspective

This review summarized different properties, preparation and structural characterization of GO nanostructured materials for degradation of organic, pollutants in wastewater. GO nanostructured materials have been successfully used for the mitigation of prominent pollutants based on the mechanism of electrostatic interaction, p – p interaction, hydrophobic interaction and hydrogen bonding. Although, graphene oxide based nanocomposites have numerous benefits, it is difficult to regenerate after usage and can lead to secondary potential pollutants when release in the environment. Hence, the need to develop green synthesis approach or magnetic ternary graphene oxide based nanocomposites for future research to solve the problem of environmental pollution and high cost of associated with the catalysts. Since instability of graphene oxide based nanocomposites can be threaten to our environment. There is a great need to ascertain the stability of any graphene oxide based nanocomposites before used and control its leakage into environment during water treatment. This can be achieved through immobilization of Graphene oxide based photocatalyst on suitable support like zeolites, glass, and stainless steel mesh among others. Hybrid AOPs are more beneficial and offer several advantages than the individual AOPs in the area of wastewater treatment. Graphene and graphene oxide derivatives should be prepared through simple and low cost environmentally friendly technique and should be applied to solve energy related crises.

Declaration of Competing Interest

The authors declare that they have no known competing financial interests or personal relationships that could have appeared to influence the work reported in this paper.

Acknowledgment

The authors acknowledged Tertiary Education Trust Fund, Nigeria, with grant number (TETF/DR&D-CE/NRF2020/SETI/116/VOL.1) for the sponsorship.

References

Lingamdinne, L.P., Koduru, J.R., Karri, R.R., 2019. A comprehensive review of applications of magnetic graphene oxide based nanocomposites for sustainable water purification. Journal of environmental management 231, 622–634.
Gupta, T., Graphene, in Carbon. 2018, Springer. p. 197-228.
Ray, S.C., 2015. Application and uses of graphene oxide and reduced graphene oxide. Applications of Graphene and Graphene-Oxide Based Nanomaterials 39–55.
Li, X., et al., 2018. Graphene-based heterojunction photocatalysts. Applied Surface Science 430, 53–107.
Vidhya, M.S., et al., 2020. Functional reduced graphene oxide/cobalt hydroxide composite for energy storage applications. Materials Letters 276, 128193.
Kumar, R., et al., 2019. Recent progress in the synthesis of graphene and derived materials for next generation electrodes of high performance lithium ion batteries. Progress in Energy and Combustion Science 75, 100786.
Kumar, R., et al., 2019. A review on synthesis of graphene, h-BN and MoS 2 for energy storage applications: Recent progress and perspectives. Nano research 12 (11), 2655–2694.
Kumar, R., et al., 2021. Recent progress on carbon-based composite materials for microwave electromagnetic interference shielding. Carbon.
Khan, Z.U., et al., 2016. A review of graphene oxide, graphene buckypaper, and polymer/graphene composites: Properties and fabrication techniques. Journal of plastic film & sheeting 32 (4), 336–379.
Kumar, R., et al., 2018. Recent advances in the synthesis and modification of carbon-based 2D materials for application in energy conversion and storage. Progress in Energy and Combustion Science 67, 115–157.
Kumar, R., et al., 2017. Laser-assisted synthesis, reduction and micro-patterning of graphene: recent progress and applications. Coordination Chemistry Reviews 342, 34–79.
Skoda, M., et al., 2014. Graphene: one material, many possibilities—application difficulties in biological systems. Journal of Nanomaterials 2014.
Yu, W., et al., 2020. Progress in the functional modification of graphene/graphene oxide: a review. RSC Advances 10 (26), 15328–15345.
Wang, J., et al., 2019. Graphene and graphene derivatives toughening polymers: Toward high toughness and strength. Chemical Engineering Journal.
Pandey, R.P., et al., 2017. Graphene oxide based nanohybrid proton exchange membranes for fuel cell applications: An overview. Advances in Colloid and Interface Science 240, 15–30.
Kumar, R., et al., 2013. Pressure-dependent synthesis of high-quality few-layer graphene by plasma-enhanced arc discharge and their thermal stability. Journal of nanoparticle research 15 (9), 1–10.
Kumar, R., et al., 2020. Heteroatom doped graphene engineering for energy storage and conversion. Materials Today 39, 47–65.
Kumar, R., et al., 2020. Microwave-assisted synthesis of Mn3O4-Fe2O3/Fe3O4@ rGO ternary hybrids and electrochemical performance for supercapacitor electrode. Diamond and Related Materials 101, 107622.
Kumar, R., et al., 2020. Honeycomb-like open-edged reduced-graphene-oxide-enclosed transition metal oxides (NiO/Co3O4) as improved electrode materials for high-performance supercapacitor. Journal of Energy Storage 30, 101539.
Hsu, K.-C., Chen, D.-H., 2014. Microwave-assisted green synthesis of Ag/reduced graphene oxide nanocomposite as a surface-enhanced Raman scattering substrate with high uniformity. Nanoscale research letters 9 (1), 1–9.
Kumar, R., et al., 2017. Controlled density of defects assisted perforated structure in reduced graphene oxide nanosheets-palladium hybrids for enhanced ethanol electro-oxidation. Carbon 117, 137–146.
Kumar, R., et al., 2021. Microwave-assisted thin reduced graphene oxide-cobalt oxide nanoparticles as hybrids for electrode materials in supercapacitor. Journal of Energy Storage 40, 102724.
Loh, K.P., et al., 2010. Graphene oxide as a chemically tunable platform for optical applications. Nature chemistry 2 (12), 1015.
Kashif, M., et al., 2021. Effect of potassium permanganate on morphological, structural and electro-optical properties of graphene oxide thin films. Arabian Journal of Chemistry 14 (2), 102953.
Xu, Z., et al., 2013. Highly electrically conductive ag-doped graphene fibers as stretchable conductors. Advanced Materials 25 (23), 3249–3253.
Gómez-Navarro, C., Burghard, M., Kern, K., 2008. Elastic properties of chemically derived single graphene sheets. Nano letters 8 (7), 2045–2049.
Robinson, J.T., et al., 2008. Wafer-scale reduced graphene oxide films for nanomechanical devices. Nano letters 8 (10), 3441–3445.
Hu, H., Onyebueke, L., Abatan, A., 2010. Characterizing and modeling mechanical properties of nanocomposites-review and evaluation. Journal of minerals and materials characterization and engineering 9 (04), 275.
Xu, Z., et al., 2013. Ultrastrong fibers assembled from giant graphene oxide sheets. Advanced Materials 25 (2), 188–193.
Xu, Z., et al., 2012. Strong, conductive, lightweight, neat graphene aerogel fibers with aligned pores. Acs Nano 6 (8), 7103–7113.
Zhao, X., et al., 2015. Graphene-based single fiber supercapacitor with a coaxial structure. Nanoscale 7 (21), 9399–9404.
Li, Z., et al., 2016. Multifunctional non-woven fabrics of interfused graphene fibres. Nature communications 7 (1), 1–11.
Fang, H., Bai, S.-L., Wong, C.P., 2016. "White graphene"–hexagonal boron nitride based polymeric composites and their application in thermal management. Composites Communications 2, 19–24.
Divya, S., Jeyadheepan, K., Hemalatha, J., 2019. Magnetoelectric P (VDF-HFP)-CoFe2O4 films and their giant magnetoresistance properties. Journal of Magnetism and Magnetic Materials 492, 165689.
Husnah, M., et al., 2017. A modified Marcano method for improving electrical properties of reduced graphene oxide (rGO). Materials Research Express 4 (6), 064001.
Prasad, S., Kumar, S.S., Shajudheen, V.M., 2020. Synthesis, characterization and study of photocatalytic activity of TiO2 nanoparticles. Materials Today: Proceedings.
Kumar, S.G., Rao, K.K., 2017. Comparison of modification strategies towards enhanced charge carrier separation and photocatalytic degradation activity of metal oxide semiconductors (TiO2, WO3 and ZnO). Applied Surface Science 391, 124–148.
Sharma, M., et al., 2018. TiO2-GO nanocomposite for photocatalysis and environmental applications: A green synthesis approach. Vacuum 156, 434–439.
Yuan, X., et al., 2018. Fabrication of ternary polyaniline-graphene oxide-TiO2 hybrid films with enhanced activity for photoelectrocatalytic hydrogen production. Separation and Purification Technology 193, 358–367.
Ahmed, A.S., et al., 2019. Removal enhancement of acid navy blue dye by GO-TiO2 nanocomposites synthesized using sonication method. Materials Chemistry and Physics 238, 121906.
Joshi, N.C., Congthak, R., Gururani, P., 2020. Synthesis, adsorptive performances and photo-catalytic activity of graphene oxide/TiO 2 (GO/TiO 2) nanocomposite-based adsorbent. Nanotechnology for Environmental Engineering 5 (3), 1–13.
Saravanan, R., Gracia, F., Stephen, A., 2017. Basic principles, mechanism, and challenges of photocatalysis. In: Nanocomposites for visible light-induced photocatalysis. Springer, pp. 19–40.
Isari, A.A., et al., 2020. Sono-photocatalytic degradation of tetracycline and pharmaceutical wastewater using WO3/CNT heterojunction nanocomposite under US and visible light irradiations: a novel hybrid system. Journal of hazardous materials 390, 122050.
Murillo-Sierra, J., et al., 2021. A review on the development of visible light-responsive WO3-based photocatalysts for environmental applications. Chemical Engineering Journal Advances 5, 100070.
Afify, H., et al., 2019. Preparation, characterization, and optical spectroscopic studies of nanocrystalline tungsten oxide WO3. Optics & Laser Technology 111, 604–611.
Basumatary, B., et al., 2022. Evaluation of Ag@ TiO2/WO3 heterojunction photocatalyst for enhanced photocatalytic activity towards methylene blue degradation. Chemosphere 286, 131848.
Yadav, A., Hunge, Y., Kang, S.-W., 2021. Porous nanoplate-like tungsten trioxide/reduced graphene oxide catalyst for sonocatalytic degradation and photocatalytic hydrogen production. Surfaces and Interfaces 24, 101075.
Malefane, M.E., et al., 2019. In-Situ Synthesis of Tetraphenylporphyrin/Tungsten (VI) Oxide/Reduced Graphene Oxide (TPP/WO3/RGO) Nanocomposite for Visible Light Photocatalytic Degradation of Acid Blue 25. ChemistrySelect 4 (29), 8379–8389.
Zhao, D., Lu, Y., Ma, D., 2020. Effects of Structure and Constituent of Prussian Blue Analogs on Their Application in Oxygen Evolution Reaction. Molecules 25 (10), 2304.
Marlinda, A., et al., 2020. Recent developments in reduced graphene oxide nanocomposites for photoelectrochemical water-splitting applications. International Journal of Hydrogen Energy 45 (21), 11976–11994.
Geraldino, H.C., et al., 2020. Electrochemical generation of H2O2 using gas diffusion electrode improved with rGO intensified with the Fe3O4/GO catalyst for degradation of textile wastewater. Journal of Water Process Engineering 36, 101377.
Song, X., et al., 2020. Fabricating C and O co-doped carbon nitride with intramolecular donor-acceptor systems for efficient photoreduction of CO2 to CO. Applied Catalysis B: Environmental 268, 118736.
Zhuang, Y., et al., 2019. Fe-Chelated polymer templated graphene aerogel with enhanced Fenton-like efficiency for water treatment. Environmental Science: Nano 6 (11), 3232–3241.
Li, D., et al., 2020. A novel Electro-Fenton process characterized by aeration from inside a graphite felt electrode with enhanced electrogeneration of H2O2 and cycle of Fe3+/Fe2+. Journal of hazardous materials 396, 122591.

Morant Giner, M., Hybrid heterostructures and materials based on transition metal dichalcogenides. 2020.
Jose, P.P.A., et al., 2018. Silver-attached reduced graphene oxide nanocomposite as an eco-friendly photocatalyst for organic dye degradation. Research on Chemical Intermediates 44 (9), 5597–5621.
Nawaz, M., et al., 2017. One-step hydrothermal synthesis of porous 3D reduced graphene oxide/TiO2 aerogel for carbamazepine photodegradation in aqueous solution. Applied Catalysis B: Environmental 203, 85–95.
Adeyanju, C.A., et al., 2022. Recent Advances on the Aqueous Phase Adsorption of Carbamazepine. ChemBioEng Reviews.
Zhang, Z., et al., 2020. Facile hydrothermal synthesis of CuO–Cu 2 O/GO nanocomposites for the photocatalytic degradation of organic dye and tetracycline pollutants. New Journal of Chemistry 44 (16), 6420–6427.
Pant, B., Park, M., Park, S.-J., 2020. Hydrothermal synthesis of Ag2CO3-TiO2 loaded reduced graphene oxide nanocomposites with highly efficient photocatalytic activity. Chemical Engineering Communications 207 (5), 688–695.
Lee, M., et al., 2015. One-step hydrothermal synthesis of graphene decorated V2O5 nanobelts for enhanced electrochemical energy storage. Scientific reports 5 (1), 1–8.
Yuan, R., et al., 2021. Supercritical CO2 Assisted Solvothermal Preparation of CoO/ Graphene Nanocomposites for High Performance Lithium-Ion Batteries. Nanomaterials 11 (3), 694.
Chin, S.J., et al., 2019. Solvothermal synthesis of graphene oxide and its composites with poly (ε-caprolactone). Nanoscale 11 (40), 18672–18682.
Yuan, W., Gu, Y., Li, L., 2012. Green synthesis of graphene/Ag nanocomposites. Applied Surface Science 261, 753–758.
Lin-jun, H., et al., 2012. Synthesis of graphene/metal nanocomposite film with good dispersibility via solvothermal method. Int J Electrochem Sci 7, 11068–11075.
Yadav, H.M., Kim, J.-S., 2016. Solvothermal synthesis of anatase TiO2-graphene oxide nanocomposites and their photocatalytic performance. Journal of Alloys and Compounds 688, 123–129.
Pu, S., et al., 2018. In situ co-precipitation preparation of a superparamagnetic graphene oxide/Fe 3 O 4 nanocomposite as an adsorbent for wastewater purification: synthesis, characterization, kinetics, and isotherm studies. Environmental Science and Pollution Research 25 (18), 17310–17320.
Ranjith, R., et al., 2019. Green synthesis of reduced graphene oxide supported TiO2/ Co3O4 nanocomposite for photocatalytic degradation of methylene blue and crystal violet. Ceramics International 45 (10), 12926–12933.
Mu, B., et al., 2017. Facile fabrication of superparamagnetic graphene/polyaniline/Fe 3 O 4 nanocomposites for fast magnetic separation and efficient removal of dye. Scientific reports 7 (1), 1–12.
Chinnathambi, A., Alahmadi, T.A., 2021. Facile synthesis of Fe3O4 anchored polyaniline intercalated graphene oxide as an effective adsorbent for the removal of hexavalent chromium and phosphate ions. Chemosphere 272, 129851.
Lee, S.H., Nishi, H., Tatsuma, T., 2017. Tunable plasmon resonance of molybdenum oxide nanoparticles synthesized in non-aqueous media. Chemical Communications 53 (94), 12680–12683.
Ma, X., et al., 2018. Fabrication of novel slurry containing graphene oxide-modified microencapsulated phase change material for direct absorption solar collector. Solar Energy Materials and Solar Cells 188, 73–80.
Pan, L., et al., 2020. Advances in Piezo-Phototronic Effect Enhanced Photocatalysis and Photoelectrocatalysis. Advanced Energy Materials 10 (15), 2000214.
Sengupta, J., Different Synthesis Routes of Graphene-Based Metal Nanocomposites. arXiv preprint arXiv:1911.01720, 2019.
Guo, X., et al., 2018. Template-assisted sol–gel synthesis of porous MoS2/C nanocomposites as anode materials for lithium-ion batteries. Journal of Sol-Gel Science and Technology 85 (1), 140–148.
Suneetha, R.B., Selvi, P., Vedhi, C., 2019. Synthesis, structural and electrochemical characterization of Zn doped iron oxide/grapheneoxide/chitosan nanocomposite for supercapacitor application. Vacuum 164, 396–404.
Zeng, X., et al., 2018. Fabrication of homogeneously dispersed graphene/Al composites by solution mixing and powder metallurgy. International Journal of Minerals, Metallurgy, and Materials 25 (1), 102–109.
Nawaz, M., et al., 2018. Photodegradation of microcystin-LR using graphene-TiO2/ sodium alginate aerogels. Carbohydrate polymers 199, 109–118.
Galpaya, D., et al., 2014. Preparation of graphene oxide/epoxy nanocomposites with significantly improved mechanical properties. Journal of Applied Physics 116 (5), 053518.
Prabhu, S., et al., 2019. Enhanced photocatalytic activities of ZnO dumbbell/reduced graphene oxide nanocomposites for degradation of organic pollutants via efficient charge separation pathway. Applied Surface Science 487, 1279–1288.
Kausar, A., et al., 2016. Perspectives of epoxy/graphene oxide composite: Significant features and technical applications. Polymer-Plastics Technology and Engineering 55 (7), 704–722.
Afzal, H.M., Mitu, S.S.I., Al-Harthi, M.A., 2018. Microwave radiations effect on electrical and mechanical properties of poly (vinyl alcohol) and PVA/graphene nanocomposites. Surfaces and Interfaces 13, 65–78.
Liu, P., Z. Yao, and J. Zhou, Preparation of reduced graphene oxide/Ni0. 4Zn0. 4Co0. 2Fe2O4 nanocomposites and their excellent microwave absorption properties. Ceramics International, 2015. **41**(10): p. 13409-13416.
Varghese, S.P., et al., 2019. Enhanced electrochemical properties of Mn3O4/graphene nanocomposite as efficient anode material for lithium ion batteries. Journal of Alloys and Compounds 780, 588–596.
Chook, S.W., et al., 2012. Antibacterial performance of Ag nanoparticles and AgGO nanocomposites prepared via rapid microwave-assisted synthesis method. Nanoscale research letters 7 (1), 541.
Seekaew, Y., et al., 2019. Synthesis, characterization, and applications of graphene and derivatives. In: Carbon-Based Nanofillers and Their Rubber Nanocomposites. Elsevier, pp. 259–283.
Borthakur, P., et al., 2016. Microwave assisted synthesis of CuS-reduced graphene oxide nanocomposite with efficient photocatalytic activity towards azo dye degradation. Journal of Environmental Chemical Engineering 4 (4), 4600–4611.
Hu, J., et al., 2017. Surfactant-assisted hydrothermal synthesis of TiO2/reduced graphene oxide nanocomposites and their photocatalytic performances. Journal of Solid State Chemistry 253, 113–120.
Banerjee, S., et al., 2018. Graphene oxide (rGO)-metal oxide (TiO2/Fe3O4) based nanocomposites for the removal of methylene blue. Applied Surface Science 439, 560–568.
Hernández-Majalca, B., et al., 2019. Visible-light photo-assisted synthesis of GO-TiO2 composites for the photocatalytic hydrogen production. International Journal of Hydrogen Energy 44 (24), 12381–12389.
Das, R.S., et al., 2019. Graphene oxide-based zirconium oxide nanocomposite for enhanced visible light-driven photocatalytic activity. Research on Chemical Intermediates 45 (4), 1689–1705.
Cheng, M.-M., et al., 2019. Synthesis of graphene oxide/polyacrylamide composite membranes for organic dyes/water separation in water purification. Journal of Materials Science 54 (1), 252–264.
Mustapha, O., Mekhzoum, M.E.M., Bouhfid, R., 2019. Surface Functionalization of Graphene-Based Nanocomposites by Chemical Reaction. In: Functionalized Graphene Nanocomposites and their Derivatives. Elsevier, pp. 21–45.
Vajedi, F.S., Dehghani, H., 2016. Synthesis of titanium dioxide nanostructures by solvothermal method and their application in preparation of nanocomposite based on graphene. Journal of materials science 51 (4), 1845–1854.
Lingamdinne, L.P., et al., 2016. Porous graphene oxide based inverse spinel nickel ferrite nanocomposites for the enhanced adsorption removal of arsenic. RSC advances 6 (77), 73776–73789.
Shan, X., et al., 2017. Surface modification of graphene oxide by goethite with enhanced tylosin photocatalytic activity under visible light irradiation. Colloids and Surfaces A: Physicochemical and Engineering Aspects 520, 420–427.
Zhang, H., et al., 2018. Synthesis and characterization of TiO 2/graphene oxide nanocomposites for photoreduction of heavy metal ions in reverse osmosis concentrate. RSC advances 8 (60), 34241–34251.
He, Y., et al., 2018. Micro-crack behavior of carbon fiber reinforced Fe3O4/graphene oxide modified epoxy composites for cryogenic application. Composites Part A: Applied Science and Manufacturing 108, 12–22.
Lingamdinne, L.P., et al., 2017. Preparation and characterization of porous reduced graphene oxide based inverse spinel nickel ferrite nanocomposite for adsorption removal of radionuclides. Journal of hazardous materials 326, 145–156.
Nejati, K., Zabihi, R., 2012. Preparation and magnetic properties of nano size nickel ferrite particles using hydrothermal method. Chemistry Central Journal 6 (1), 23.
Liu, Y., et al., 2017. Enhanced catalytic degradation of methylene blue by α-Fe2O3/ graphene oxide via heterogeneous photo-Fenton reactions. Applied Catalysis B: Environmental 206, 642–652.
Perez, J.V.D., et al., 2017. Response surface methodology as a powerful tool to optimize the synthesis of polymer-based graphene oxide nanocomposites for simultaneous removal of cationic and anionic heavy metal contaminants. RSC advances 7 (30), 18480–18490.
Nwosu, F.O., et al., 2018. Preparation and characterization of adsorbents derived from bentonite and kaolin clays. Applied Water Science 8 (7), 195.
Zhang, B., et al., 2020. Fabricating ZnO/lignin-derived flower-like carbon composite with excellent photocatalytic activity and recyclability. Carbon 162, 256–266.
Mohanta, J., Dey, B., Dey, S., 2020. Highly Porous Iron-Zirconium Binary Oxide for Efficient Removal of Congo Red from Water. Desalin. Water, Treat.
Thangavel, S., et al., 2016. Designing ZnS decorated reduced graphene-oxide nanohybrid via microwave route and their application in photocatalysis. Journal of Alloys and Compounds 683, 456–462.
Kashinath, L., Namratha, K., Byrappa, K., 2017. Sol-gel assisted hydrothermal synthesis and characterization of hybrid ZnS-RGO nanocomposite for efficient photodegradation of dyes. Journal of Alloys and Compounds 695, 799–809.
Gerassimidou, S., et al., 2020. Characterisation and composition identification of waste-derived fuels obtained from municipal solid waste using thermogravimetry: A review. Waste Management & Research 38 (9), 942–965.
Alacoque, D., Combustion properties of reclaimed used engine lubricating oil blended with salmon fish oil and woody pyrolysis oil. 2018, Memorial University of Newfoundland.
Nikitin, A., et al., 2021. Anthropogenic emissions from the combustion of composite coal-based fuels. Science of The Total Environment 772, 144909.
Fan, H., 2019. Fluorinated functionalization of graphene oxide and its role as a reinforcement in epoxy composites. Journal of Polymer Research 26 (2), 1–12.
Shao, F., Zenobi, R., 2019. Tip-enhanced Raman spectroscopy: principles, practice, and applications to nanospectroscopic imaging of 2D materials. Analytical and bioanalytical chemistry 411 (1), 37–61.
Kumar, S., et al., 2020. Surface-Enhanced Raman Scattering: Introduction and Applications. In: Recent Advances in Nanophotonics-Fundamentals and Applications. IntechOpen London, UK, pp. 1–24.
Sharma, N., et al., 2019. A new sustainable green protocol for production of reduced graphene oxide and its gas sensing properties. Journal of Science: Advanced Materials and Devices 4 (3), 473–482.
Miklos, D.B., et al., 2018. Evaluation of advanced oxidation processes for water and wastewater treatment–A critical review. Water research 139, 118–131.

Ighalo, J.O., et al., 2021. CuO Nanoparticles (CuO NPs) for Water Treatment: A Review of Recent Advances. Environmental Nanotechnology, Monitoring & Management, 100443.
Zhang, M.-H., et al., 2019. A review on Fenton process for organic wastewater treatment based on optimization perspective. Science of the total environment.
Akyol, A., et al., 2019. Treatment of phenol formaldehyde production wastewater by electrooxidation-electrofenton successive processes. Separation Science and Technology 1–14.
Garcia-Muñoz, P., et al., 2020. Synergy effect between photocatalysis and heterogeneous photo-Fenton catalysis on Ti-doped LaFeO 3 perovskite for high efficiency light-assisted water treatment. Catalysis Science & Technology 10 (5), 1299–1310.
Xu, L., et al., 2020. Degradation of emerging contaminants by sono-Fenton process with in situ generated H2O2 and the improvement by P25-mediated visible light irradiation. Journal of Hazardous Materials 391, 122229.
Alcaide, F., et al., 2020. A stable CoSP/MWCNTs air-diffusion cathode for the photoelectro-Fenton degradation of organic pollutants at pre-pilot scale. Chemical Engineering Journal 379, 122417.
Tanatti, N.P., et al., 2019. Kinetics and thermodynamics of biodiesel wastewater treatment by using ozonation process. Desalination and Water Treatment 161, 108–115.
Dutta, A., et al., 2017. Sunlight-assisted photo-fenton process for removal of insecticide from agricultural wastewater. In: Trends in Asian Water Environmental Science and Technology. Springer, pp. 23–33.
Soltani, T., Lee, B.-K., 2017. Enhanced formation of sulfate radicals by metal-doped BiFeO3 under visible light for improving photo-Fenton catalytic degradation of 2-chlorophenol. Chemical Engineering Journal 313, 1258–1268.
Nidheesh, P., Rajan, R., 2016. Removal of rhodamine B from a water medium using hydroxyl and sulphate radicals generated by iron loaded activated carbon. RSC advances 6 (7), 5330–5340.
Zubir, N.A., Graphene oxide-iron oxide nanocomposites for dye contaminated wastewater remediation. 2015.
Deng, Y., Zhao, R., 2015. Advanced oxidation processes (AOPs) in wastewater treatment. Current Pollution Reports 1 (3), 167–176.
Gopal, G., et al., 2020. A review on tetracycline removal from aqueous systems by advanced treatment techniques. RSC Advances 10 (45), 27081–27095.
Fujishima, A., Honda, K., 1972. Electrochemical photolysis of water at a semiconductor electrode. nature 238 (5358), 37–38.
Frank, S.N., Bard, A.J., 1977. Heterogeneous photocatalytic oxidation of cyanide ion in aqueous solutions at titanium dioxide powder. Journal of the American Chemical Society 99 (1), 303–304.
Norhayati, H., et al., 2016. A Brief Review On Recent Graphene Oxide-Based Material Nanoco Mposites. Synthesis And Applications.
Solis-Casados, D., et al., 2018. Advanced Oxidation Processes II: Removal of pharmaceuticals by photocatalysis. In: Ecopharmacovigilance. Springer, pp. 143–155.
Zhang, J., et al., 2017. Carbon nanodots/WO3 nanorods Z-scheme composites: remarkably enhanced photocatalytic performance under broad spectrum. Applied Catalysis B: Environmental 209, 253–264.
Bhanvase, B., Shende, T., Sonawane, S., 2017. A review on graphene–TiO2 and doped graphene–TiO2 nanocomposite photocatalyst for water and wastewater treatment. Environmental Technology Reviews 6 (1), 1–14.
Ashouri, R., et al., 2019. The effect of ZnO-based carbonaceous materials for degradation of benzoic pollutants: a review. International Journal of Environmental Science and Technology 16 (3), 1729–1740.
Kumar, A.S.K., Jiang, S.-J., 2017. Synthesis of magnetically separable and recyclable magnetic nanoparticles decorated with β-cyclodextrin functionalized graphene oxide an excellent adsorption of As (V)/(III). Journal of Molecular Liquids 237, 387–401.
Chowdhury, S., Balasubramanian, R., 2014. Recent advances in the use of graphene-family nanoadsorbents for removal of toxic pollutants from wastewater. Advances in colloid and interface science 204, 35–56.
Khan, M., et al., 2015. Graphene based metal and metal oxide nanocomposites: synthesis, properties and their applications. Journal of Materials Chemistry A 3 (37), 18753–18808.
Tayel, A., Ramadan, A.R., El Seoud, O.A., 2018. Titanium dioxide/graphene and titanium dioxide/graphene oxide nanocomposites: Synthesis, characterization and photocatalytic applications for water decontamination. Catalysts 8 (11), 491.
Zheng, X., et al., 2013. Titanium dioxide photonic crystals with enhanced photocatalytic activity: Matching photonic band gaps of TiO2 to the absorption peaks of dyes. The Journal of Physical Chemistry C 117 (41), 21263–21273.
Ajala, O.J., et al., 2022. Wastewater Treatment Technologies. In: Inorganic-Organic Composites for Water and Wastewater Treatment. Springer, pp. 1–28.
Cao, M., et al., 2016. Visible light activated photocatalytic degradation of tetracycline by a magnetically separable composite photocatalyst: graphene oxide/magnetite/cerium-doped titania. Journal of colloid and interface science 467, 129–139.
Priya, B., et al., 2016. Adsorptional photocatalytic mineralization of oxytetracycline and ampicillin antibiotics using Bi2O3/BiOCl supported on graphene sand composite and chitosan. Journal of colloid and interface science 479, 271–283.
Hu, X.-Y., et al., 2016. Graphene/TiO2/ZSM-5 composites synthesized by mixture design were used for photocatalytic degradation of oxytetracycline under visible light: Mechanism and biotoxicity. Applied surface science 362, 329–334.
Priya, B., et al., 2016. Photocatalytic mineralization and degradation kinetics of ampicillin and oxytetracycline antibiotics using graphene sand composite and chitosan supported BiOCl. Journal of Molecular Catalysis A: Chemical 423, 400–413.
Jo, W.-K., et al., 2017. Cobalt promoted TiO2/GO for the photocatalytic degradation of oxytetracycline and Congo Red. Applied Catalysis B: Environmental 201, 159–168.
Bai, J., et al., 2017. Facile preparation 3D ZnS nanospheres-reduced graphene oxide composites for enhanced photodegradation of norfloxacin. Journal of Alloys and Compounds 729, 809–815.
Anirudhan, T., Deepa, J., 2017. Nano-zinc oxide incorporated graphene oxide/nanocellulose composite for the adsorption and photo catalytic degradation of ciprofloxacin hydrochloride from aqueous solutions. Journal of colloid and interface science 490, 343–356.
Yang, C., et al., 2017. A novel visible-light-driven In-based MOF/graphene oxide composite photocatalyst with enhanced photocatalytic activity toward the degradation of amoxicillin. Applied Catalysis B: Environmental 200, 673–680.
Karaolia, P., et al., 2018. Removal of antibiotics, antibiotic-resistant bacteria and their associated genes by graphene-based TiO2 composite photocatalysts under solar radiation in urban wastewaters. Applied Catalysis B: Environmental 224, 810–824.
Tang, X., Wang, Z., Wang, Y., 2018. Visible active N-doped TiO2/reduced graphene oxide for the degradation of tetracycline hydrochloride. Chemical Physics Letters 691, 408–414.
Chakraborty, K., Pal, T., Ghosh, S., 2018. RGO-ZnTe: A graphene based composite for tetracycline degradation and their synergistic effect. ACS Applied Nano Materials 1 (7), 3137–3144.
Appavu, B., et al., 2018. BiVO4/N-rGO nano composites as highly efficient visible active photocatalyst for the degradation of dyes and antibiotics in eco system. Ecotoxicology and environmental safety 151, 118–126.
Shabani, M., et al., 2019. Sono-solvothermal hybrid fabrication of BiOCl-Bi24O31Cl10/rGO nano-heterostructure photocatalyst with efficient solar-light-driven performance in degradation of fluoroquinolone antibiotics. Solar Energy Materials and Solar Cells 193, 335–350.
Shaniba, C., et al., 2020. Sunlight-assisted oxidative degradation of cefixime antibiotic from aqueous medium using TiO2/nitrogen doped holey graphene nanocomposite as a high performance photocatalyst. Journal of Environmental Chemical Engineering 8 (1), 102204.
Kumar, S., Kaushik, R., Purohit, L., 2022. ZnO-CdO nanocomposites incorporated with graphene oxide nanosheets for efficient photocatalytic degradation of bisphenol A, thymol blue and ciprofloxacin. Journal of Hazardous Materials 424, 127332.
Zhao, Y., et al., 2022. Reduced graphene oxide supported ZnO/CdS heterojunction enhances photocatalytic removal efficiency of hexavalent chromium from aqueous solution. Chemosphere 286, 131738.
Nisar, A., et al., 2022. Synthesis and characterization of ZnO decorated reduced graphene oxide (ZnO-rGO) and evaluation of its photocatalytic activity toward photodegradation of methylene blue. Environmental Science and Pollution Research 29 (1), 418–430.
Wu, P., et al., 2021. Flower-like FeOOH hybridized with carbon quantum dots for efficient photo-Fenton degradation of organic pollutants. Applied Surface Science 540, 148362.
Xavier, S., et al., 2016. Comparative removal of Magenta MB from aqueous solution by homogeneous and heterogeneous photo-Fenton processes. Desalination and Water Treatment 57 (27), 12832–12841.
Xie, A., et al., 2020. Graphene oxide/Fe (III)-based metal-organic framework membrane for enhanced water purification based on synergistic separation and photo-Fenton processes. Applied Catalysis B: Environmental 264, 118548.
Lin, F., et al., 2019. Advanced asymmetric supercapacitor based on molybdenum trioxide decorated nickel cobalt oxide nanosheets and three-dimensional α-FeOOH/rGO. Electrochimica Acta 320, 134580.
Gopi, C.V.M., et al., 2020. Co9S8-Ni3S2/CuMn2O4-NiMn2O4 and MnFe2O4-ZnFe2O4/graphene as binder-free cathode and anode materials for high energy density supercapacitors. Chemical Engineering Journal 381, 122640.
Lu, Y., et al., 2016. Synthesis of sulfur/FePO4/graphene oxide nanocomposites for lithium–sulfur batteries. Ceramics International 42 (9), 11482–11485.
Yu, L., et al., 2016. Degradation of phenol using Fe3O4-GO nanocomposite as a heterogeneous photo-Fenton catalyst. Separation and Purification Technology 171, 80–87.
Nguyen, X.S., Zhang, G., Yang, X., 2017. Mesocrystalline Zn-doped Fe3O4 hollow submicrospheres: formation mechanism and enhanced photo-Fenton catalytic performance. ACS applied materials & interfaces 9 (10), 8900–8909.
Wan, Z., Wang, J., 2017. Degradation of sulfamethazine using Fe3O4-Mn3O4/reduced graphene oxide hybrid as Fenton-like catalyst. Journal of Hazardous Materials 324, 653–664.
Zhu, Y., et al., 2018. Heterogeneous photo-Fenton degradation of bisphenol A over Ag/AgCl/ferrihydrite catalysts under visible light. Chemical Engineering Journal 346, 567–577.
Jiang, Z., et al., 2019. Photo-Fenton degradation of phenol by CdS/rGO/Fe2+ at natural pH with in situ-generated H2O2. Applied Catalysis B: Environmental 241, 367–374.
Heidari, M.R., et al., 2019. Photo-fenton like catalyst system: activated carbon/CoFe2O4 nanocomposite for reactive dye removal from textile wastewater. Applied Sciences 9 (5), 963.
Wu, J., et al., 2022. UV-assisted nitrogen-doped reduced graphene oxide/Fe3O4 composite activated peroxodisulfate degradation of norfloxacin. Environmental Technology 43 (1), 95–106.
Kumar, G., Dutta, R.K., 2022. Sunlight mediated photo-Fenton degradation of tetracycline antibiotic and methylene blue dye in aqueous medium using FeWO4/Bi2MoO6 nanocomposite. Process Safety and Environmental Protection.
Muruganandham, M., et al., 2014. Recent developments in homogeneous advanced oxidation processes for water and wastewater treatment. International Journal of Photoenergy 2014.
Kumar, S.G., Kavitha, R., Nithya, P., 2020. Tailoring the CdS surface structure for photocatalytic applications. Journal of Environmental Chemical Engineering 8 (5), 104313.

Chávez, A.M., Solís, R.R., Beltrán, F.J., 2020. Magnetic graphene TiO2-based photocatalyst for the removal of pollutants of emerging concern in water by simulated sunlight aided photocatalytic ozonation. Applied Catalysis B: Environmental 262, 118275.

Chakma, S., et al., 2020. Investigation in sono-photocatalysis process using doped catalyst and ferrite nanoparticles for wastewater treatment. In: Nanophotocatalysis and environmental applications. Springer, pp. 171–194.

Heidarizad, M., Şengör, S.S., 2017. 2017.. Graphene Oxide/Magnesium Oxide Nanocomposite: A Novel Catalyst for Ozonation of Phenol from Wastewater. in World Environmental and Water Resources Congress.

Govindasamy, M., et al., 2019. Facile sonochemical synthesis of perovskite-type SrTiO3 nanocubes with reduced graphene oxide nanocatalyst for an enhanced electrochemical detection of α-amino acid (tryptophan). Ultrasonics sonochemistry 56, 193–199.

Nirumand, L., et al., 2018. Synthesis and sonocatalytic performance of a ternary magnetic MIL-101 (Cr)/RGO/ZnFe2O4 nanocomposite for degradation of dye pollutants. Ultrasonics sonochemistry 42, 647–658.

Ayoubi-Feiz, B., Mashhadizadeh, M.H., Sheydaei, M., 2019. Degradation of diazinon by new hybrid nanocomposites N-TiO2/Graphene/Au and N-TiO2/Graphene/Ag using visible light photo-electro catalysis and photo-electro catalytic ozonation: Optimization and comparative study by Taguchi method. Separation and Purification Technology 211, 704–714.

Vinesh, V., Shaheer, A., Neppolian, B., 2019. Reduced graphene oxide (rGO) supported electron deficient B-doped TiO2 (Au/B-TiO2/rGO) nanocomposite: an efficient visible light sonophotocatalyst for the degradation of Tetracycline (TC). Ultrasonics sonochemistry 50, 302–310.

Liu, J., Wang, Y., Wang, L., 2019. Poly (3, 4-ethylenedioxythiophene) modified polyvinylidene fluoride membrane for visible photoelectrocatalysis and filtration. Journal of colloid and interface science 553, 220–227.